VOL. 1 No. 12 DECEMBER 1936

Philips Technical Review

DEALING WITH TECHNICAL PROBLEMS
RELATING TO THE PRODUCTS, PROCESSES AND INVESTIGATIONS OF
N.V. PHILIPS' GLOEILAMPENFABRIEKEN

EDITED BY THE RESEARCH LABORATORY OF N.V. PHILIPS' GLOEILAMPENFABRIEKEN, EINDHOVEN, HOLLAND

HOW CAN ONE JUDGE THE EFFICIENCY OF ROAD LIGHTING?

By G. HOLST and P. J. BOUMA.

Summary. To determine the efficiency of road lighting equipment neither a knowledge of the illumination intensity nor information of the brightness distribution on the highway is sufficient in itself. It is necessary to carry out in addition visibility measurements directly on the highway in question. Following a discussion of the fundamental principles which a visibility meter has to satisfy, a simple type of instrument is described. The results of measurements for different existing lighting equipments are given and discussed.

Introduction

In a number of previous articles [1]) we have discussed various characteristics of the eye which throw light on the mechanism of perception of objects on a highway and indicate the factors which affect the ability of perception either favourably or adversely. In addition, these data bring out the general principles governing the design of lighting equipment.

Our knowledge of the mechanism of vision has by no means advanced to such a stage that from the characteristics of the eye we can without further ado evolve the ideal method of illumination for a particular case. In the first place, we frequently do not know to what extent the various factors entailed, such as the visual acuity, contrast sensitivity, etc., contribute to visual perception, and moreover in every system of road lighting there are various associated factors (such as the brightness conditions of the surroundings, alterations in the reflecting powers of the road, as a result of wear and moisture), whose effect on the ability of perception it is difficult to estimate.

Both to extend our practical knowledge as well as to permit expression of the intrinsic value of a specific lighting system in practice, it is therefore extremely desirable to be able to make a reliable evaluation of the efficiency of a lighting equipment already in service and if at all possible to express its characteristics numerically.

It must be clearly emphasised that to do this measurements made on the highway itself are absolutely indispensable, for only by performing such a survey can all factors which determine perception on the highway be included in the results of measurement. Measurements made on reduced scale models of an equipment or a study of photographs and films of the illuminated highway are usually quite inadequate for this purpose.

Measurement of the Intensity of Illumination

What measurements must be conducted on the highway in order to arrive at useful and reliable values expressing the quality or efficiency of the lighting equipment?

In the past, illumination surveys were frequently limited to a measurement of the horizontal and vertical illumination, i.e. to a measurement of the amount of light, incident on different areas of the road surface and on different vertical surfaces. It is evident that such illumination measurements really give no information as to how well the eye can perceive objects. What interests us is by no means the quantity of light falling on various road areas or on the objects on the highway which we have to perceive, but rather the quantity of light which the different parts of the road and the objects radiate in the direction of our eyes and which is utilised for visual perception. In other words: It is less a question of the intensity of illumination of the highway as of the brightness. If two different roads are equipped with the same type of lamps, the results obtained can yet differ considerably, if one road surface has entirely different properties of reflection than the other (e.g. is darker or has a greater specular reflection); although the intensities of illumination are the same, the distribution of brightness is different.

[1]) Philips techn. Rev. 1, 102, 142, 166, 215, 225, 1936.

Measurement of Brightness

We can thus judge the quality of the illumination much better by measuring the brightness values instead of the intensity of illumination on the highway.

A practical difficulty is encountered in that the requisite measurements are very tedious. For while the intensity of illumination at a specific point on the road can be obtained by a single measurement, the brightness of the same area of surface is different in different directions, i.e. it depends on the location of the observer. To make a complete survey of the brightness conditions it therefore becomes necessary not only to move our measuring instrument in succession to all parts of the road surface, but the observer himself has also to take up various positions.

A serious disadvantage of a more fundamental character is that a determination of the brightness distribution over the roadway does not yet give the necessary answer to the question as to how well we can see on the highway. There are several reasons for this.

In the first place, perception is not determined exclusively by the brightness values of the roadway and of the objects located on it, but may also depend e.g. on the presence of sources of glare: Brightness measurements alone therefore do not afford an adequate basis for judging the lighting. At the same time they provide certain data in a not-readily usuable form, for it is difficult, if not impossible, to deduce from the distribution of brightness the efficiency of vision on the highway. It is indeed possible to determine from brightness measurements, for instance, whether the highway has any bright and dark spots or not, but it is not easy to estimate the effect of this irregularity on the facility of perception.

Measurement of Visual Performances

It is seen that nothing else remains but to conduct experiments on the highway of the visibility of the objects on it.

If a number of different objects are placed at different points on a highway and it is estimated at what distance they are still perceptible or recognisable a true idea is obtained of the visibility of such objects on the highway, although the measurements themselves are very cumbersome, tedious and frequently dangerous. It is therefore important to investigate whether these experiments can be facilitated by means of an optical instrument.

In designing such an instrument, the fundamental requirement must not be lost sight of that in observations with it the eye must function under exactly the same conditions as when perception is performed with the naked eye. If there is any divergence from this equivalence, we still measure the performances of the eye, yet it will be functioning under conditions which do not occur in practice.

Practically every measurement of visual performance is based on determining a "threshold value", i.e. a determination of the conditions under which the eye can still just perceive a particular object. The first question which arises is therefore: How can we create the conditions required for determining the requisite threshold value?

The most direct way appears to be to reduce the brightness of the whole field of vision — e.g. by placing light-absorbing glasses in front of the eyes — to such a value that a test object on the highway becomes invisible, and to take the magnitude of this brightness reduction as a measure of the visibility of the object in question. An instrument [2]) extensively used in America functions on this principle, but it is apparent that this method does not satisfy the fundamental requirement stated above, for in using the instrument the eye is functioning under conditions — in this case at brightness values — which never occur in practice on the highway concerned. This divergence can in many cases readily result in an entirely false evaluation of the quality of the lighting system. The greatest danger of this is incurred when the method is employed to compare the illumination values produced by different types of light sources. As has already been discussed in detail [3]), the brightness level is a factor of paramount importance in making such comparisons: A system of lighting which proves efficient at the brightness levels occurring on the highway may prove less favourable than another method of lighting at low brightness values. The effect of glare on perception in general also does not remain the same if the brightness of the highway surface and of the source of glare are reduced by the same factor.

A better method for determining the threshold values is offered by making the test object variable or by selecting the still just visible test object out of a group of these objects. Since setting up a group of test objects on a roadway is a very cumbersome and time-wasting procedure, an apparatus has been devised in which a lens throws an image of

---

[2]) The "visibility meter" of Luckiesh (J. Frank. Inst., **220**, 431, 1935).

[3]) Philips techn. Rev. **1**, 166, 1936.

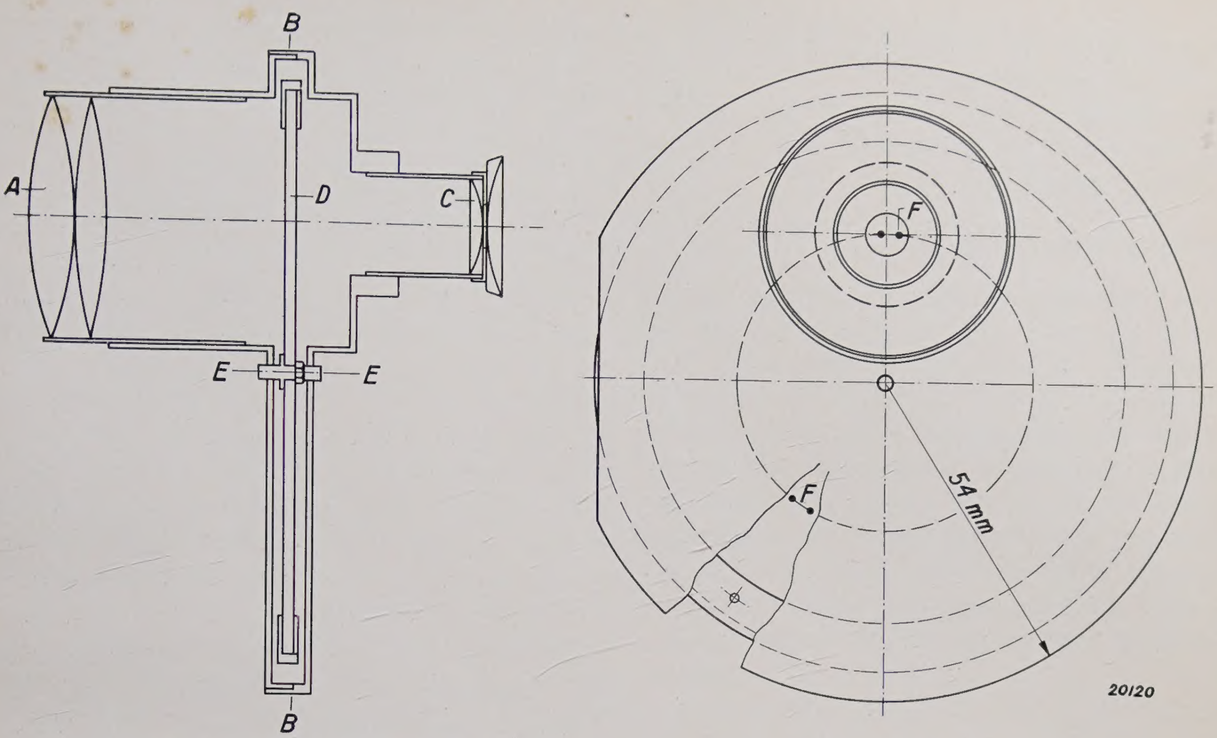

Fig. 1. "Philips Visibility Meter". *A* objective and *C* lens, with which the spots *F* with progressively increasing transmission coefficients are observed against the road surface as background.

the road on to a plane in front of the eyepiece, and in which the test objects are also located.

Construction of the "Philips Visibility Meter"

Fig. 1 shows the construction of an apparatus designed by us on this principle. The objective *A* projects an image of the highway surface on the plane *B-B*, in which a glass disc *D* pivoted about the axis *E-E* is mounted. On the disc there are 50 small numbered circular spots *F* with different transmission coefficients which have been prepared by photographic means. These spots are viewed together with the image of the roadway through the lens *C*. Directing the instrument towards the area of road under investigation and turning the disc *D*, the spot which is still just perceptible against the highway as background can be determined.

In the practical design of this apparatus the fundamental requirement stated was to a large intent satisfied, viz., that the eye when using the instrument should function under exactly the same conditions as in normal vision. The following points are important in this respect:

1) On a highway objects nearly always appear dark against the background of the surface; the same contrast is found with the test objects.
2) To avoid sources of glare, which affect perception to a marked extent, from being screened off during observation, the field of vision has been made very large. That this reduces the definition at the edges of the image is of secondary importance.
3) The angles of vision between different objects in the field of view, for instance between an object being perceived and a source of glare, must not be altered by the instrument. This has been achieved by adopting the same focal length for *A* and *C*, as a result of which the whole optical system has a magnification of 1 : 1.
4) The angular dimensions of the test objects must be of the same order of magnitude as the obstructions present on the roadway. In the apparatus described the spots subtend an angle of about 35′, which is equivalent to the angle subtended by a pedestrian seen at a distance of about 150 yards.
5) The contrasts between the test object and the background must be comparable to those actually occurring on a highway.

Fig. 2 illustrates the calibration of one of the glass plates used. Along the abscissa the numbers of the spots *N* are plotted, and along this ordinate the contrast *K* [4]) which the spot exhibits against

---

[4]) The contrast between two brightness values is defined as:

$$K = \frac{\text{Maximum brightness} - \text{minimum brightness}}{\text{maximum brightness}}.$$

A spot with the transmission coefficient p thus produces a contrast of $K = 1 - p$.

the road surface as background. The contrasts lie between 80 per cent (an object with a reflecting power one fifth of that of the road) and 2 per cent (a contrast just still perceptible under the most favourable conditions).

Results of Measurements

The values measured naturally differ for different areas of the road surface (irregularity in brightness distribution, variable effect of glare, etc.). If we determine the highest and the lowest values for a particular highway, we shall in fact already obtain a fairly reliable picture of the efficiency of the lighting, at any rate a better idea than would be got by a complete survey of the illumination intensities or the brightness distribution.

Table I gives the results of some measurements carried out on existing lighting systems.

Table I

	Place	Type of Lighting	Installed power kW/km	Just perceptible contrast: Most favour able	Most unfavour able	Average
1	Eindhoven	Sodium	3	0.07	0.20	0.14
2	Cheltenham	,,	2.5			0.15
3	Vught	,,	3			0.10
4	Croydon [5])	,,	4.3			0.15
5	Vught	Blended light [6])	6.3			0.18
6	London	Mercury	10.5			0.34
7	Cheltenham	,,	9.5			0.39
8	Eindhoven	Glow lamps	5	0.19	0.31	0.25
9	,,	,,		0.34	0.47	0.40
10	Eindhoven	Gas lamps		0.39	0.70	0.54
11	London	,,				0.28
4a	Croydon	Sodium	4.3	With glare source		0.34

The following points are of interest in connection with these measurements:

The results 1 - 4 obtained on different highways illuminated by sodium are in surprisingly good agreement, while those obtained for the three roadways lighted with mercury (5 - 7) differ considerably from each other, the reason for which is immediately apparent; In the lighting system at Vught provision is made by using socalled concentrated reflectors so that the lamps radiate no

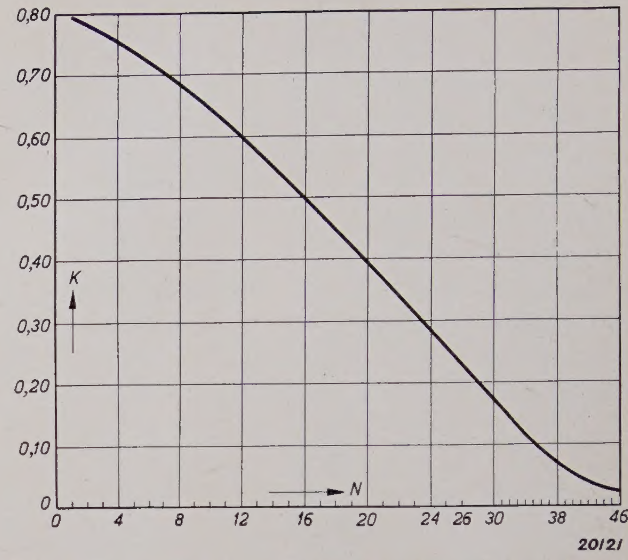

Fig. 2. The contrast K of the spots numbered from 1 to 46 against their background.

light at an angle close to the horizontal, while such concentration is not employed in the other systems (distributing or dispersive reflectors). The marked difference between 5, 6 and 7 is therefore mainly due to glare resulting from the pronounced radiation of light in an almost horizontal direction.

Examples 8 and 9 relate to the best and the worst of a number of lighted roadways equipped with ordinary electric lamps in the vicinity of Eindhoven, while examples 10 and 11 refer to an inefficient and a satisfactory gas lighting equipment respectively.

Example 4a applies to the same equipment as 4, but measurements were made at a moment when a motor vehicle with headlights on appeared in the field of vision at a distance of approx. 200 yards. It is seen that glare has had a pronounced adverse effect on visibility.

The best visibility values are obviously obtained with sodium and mercury lighting systems (1 - 5) if the sources are screened from direct exposure to the eye; it should be noted how this result has been achieved with a low current consumption in kilowatts per kilometer.

The general observation should be noted that the illumination is inadequate for fast traffic when contrasts of approx. 25 per cent can no longer be perceived over greater parts of the road surface. The requirements as regards fast traffic are therefore only fully met by lighting equipments 1 - 5. (where example 4a demonstrates how necessary it becomes to traverse such well-lighted roadways with screened headlights), while the best glow lamp and gas lighting systems (8 and 11) lie just at the boundary.

---

[5]) See photograph on p. 312 in the October issue of Philips techn. Rev.

[6]) We call blended light a mixture of mercury light and glow lamps.

THE USE OF LOADING COILS IN TELEPHONY

By W. SIX.

Summary. The attention effects and distortions obtained in a telephone cable can be appreciably reduced by the insertion of induction coils (termed Pupin or loading coils) in the line at regular intervals. In this article it is shown on the basis of the theory of coil-loaded conductors that the iron cores of the loading coils have to possess the following characteristics: High permeability, low hysteresis, and high stability. By a combined rolling and heat-treatment process it has been possible to produce nickel-iron strip which adequately satisfies these requirements.

In telephone circuits the sound waves are converted by the microphone into electric waves which are transmitted by conductors and then re-converted into sound waves by the telephone receiver.

The sound waves generated by the human voice are composed of vibrations of various frequencies with extremely divergent amplitudes. Satisfactory transmission is only realised when the sound waves generated by the telephone receiver contain the different frequencies in the same mutual ratios of intensity as the sound waves picked up by the microphone. On the other hand, the ear is fairly insensitive to alterations in the phase of the individual vibrations. In a telephone circuit consisting of microphone, conductor and receiver, each of these three components affects transmission in some way or other. In the present article attention will be limited to the conductors alone. Fortunately the human ear is capable of detecting the originating sound, even in a highly-distorted sound complex. On a marked change in the ratios of the amplitudes, the tone is however altered; thus the voice sounds drummy when high-frequency vibrations have a lower amplitude than low-frequency vibrations. Yet if the higher frequencies become too attenuated, there will eventually remain only a heavy hum and speech will become quite unintelligible.

As will be shown in greater detail later, the attenuation of the line or conductor causes a reduction in the amplitude of a sinusoidal electric vibration traversing the line. The attenuation increases with the frequency. Moreover, the velocity of propagation is smaller for higher frequencies than for lower frequencies, with the net result that in the transmission of compound vibrations along the line the composition of these vibrations will vary with the attenuation and the alteration in phase. This phenomenon proved a serious obstacle in the early days of telephony to the setting up of efficient telephone channels.

In addition to its electrical resistance, a telephone line, whether in the form of a buried cable or an overhead line, also possesses capacity, self-induction and leakance. A conductor of this type can be simulated by a network with series impedances composed of resistance and self-induction and with parallel reactances composed of capacity and leakance.

In *fig. 1* the substitution scheme of a unit length

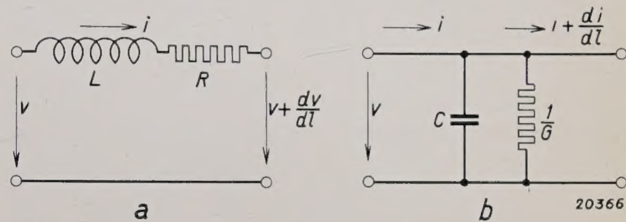

Fig. 1. Substitution diagram for a unit length of a cable.
a) Effect of resistance and self-induction on the voltages in the cable.
b) Effect of leakance and capacity on the currents.

of cable is shown diagrammatically. From a study of this diagram the following differential equations, which state how the current i and the voltage v vary with the longitudinal co-ordinate l of the cable, can be derived:

$$\left.\begin{aligned} -\frac{\partial v}{\partial l} &= R\,i + L\frac{\partial i}{\partial t} \\ -\frac{\partial i}{\partial l} &= G\,v + C\frac{\partial v}{\partial t} \end{aligned}\right\} \quad \ldots \ldots (1)$$

where R is the resistance, L the self-induction, C the capacity and G the leakance per km of cable.

To solve these equations the voltages and currents assumed to be sinusoidal are expressed as complex functions of the time:

$$i = I\,e^{j\,\omega t}$$

$$v = V e^{j\,\omega t}$$

We can then write the above differential equations as follows:

$$\left.\begin{aligned} -\frac{\partial V}{\partial l} &= (R + j\omega L)\, I \\ -\frac{\partial I}{\partial l} &= (G + j\omega C)\, V \end{aligned}\right\} \quad . \; . \; . \quad (2)$$

These equations are satisfied by:

$$V = V_0\, e^{-Tl},$$
$$I = I_0\, e^{-Tl},$$

where I_0 and V_0 are the current and voltage at the input of the line and:

$$T = \sqrt{(R + j\omega L)\,(G + j\omega C)} = \alpha + j\beta \quad . \quad (3)$$

T is termed the propagation constant and is compounded of a real component α, the attenuation constant, and an imaginary component $j\beta$, the phase constant. Voltage and current along the line are expressed by the following:

$$v = V e^{j\omega t} = V_0\, e^{-(\alpha+j\beta)l}\, e^{j\omega t},$$

$$\left.\begin{aligned} v &= V_0\, e^{-\alpha l}\, e^{j\omega\,(t-\beta l/\omega)} \\ i &= I_0\, e^{-\alpha l}\, e^{j\omega\,(t-\beta l/\omega)} \end{aligned}\right\} \quad . \; . \; . \quad (4)$$

It follows from this form of expression that the voltage and the current are propagated along the line in the form of attenuated or damped travelling waves. The attenuation is determined by α. The velocity of propagation is:

$$S = \frac{\omega}{\beta}$$

If the real parts on both sides of equation (3) are equated to each other, as well as the imaginary parts, we get:

$$\alpha = \sqrt{{}^1/_2 \sqrt{(R^2+\omega^2L^2)\,(G^2+\omega^2C^2)} + {}^1/_2\,(RG - \omega^2 LC)}$$

$$\beta = \sqrt{{}^1/_2 \sqrt{(R^2+\omega^2L^2)\,(G^2+\omega^2C^2)} - {}^1/_2\,(RG - \omega^2 LC)}.$$

Lack of knowledge of the theory of propagation of electric vibrations along conductors, which has been briefly outlined above, was responsible for the initial failure to arrive at reliable and efficient telephone channels. It was indeed rapidly realised that the attenuation increased with the resistance and the capacity, although at the same time it was generally assumed that the principal requirement was to keep the self-induction of the line as low as possible.

In 1887 Heaviside developed the theory of propagation of electrical vibrations along conductors, and at the same time showed that the comparatively complex formulae for the propagation constant became much simplified in the special case of $LG = RC$. Then $\alpha = \sqrt{RG}$ and $\beta = \omega\sqrt{LC}$. The velocity of propagation S in this case becomes:

$$S = \frac{\omega}{\beta} = \frac{1}{\sqrt{LC}}$$

In a conductor satisfying this condition both the attenuation and the velocity of propagation are thus independent of the frequency, in other words a vibration compounded of a variety of frequencies can also be transmitted along the line without any distortion whatsoever being created. Although the train of waves is damped here also, yet the form of the train remains unchanged. The line is then said to be distortionless or non-distorting.

Since in normal types of cable RC is always considerably greater than LG, the question arises how the condition $LG = RC$ can be satisfied. It is possible, firstly, to make R or C smaller, and indeed it is known that the attenuation in low-capacity overhead lines is considerably smaller than that of cables and that also by increasing the cross-section of the conductor, i.e. by reducing the resistance, the attenuation can be diminished. But all possibilities in this direction have already been exhausted within commercial limits.

Secondly, it would appear possible to arrive at distortionless lines by increasing G or L. Increasing G does indeed result in making the attenuation the same for all frequencies, but also produces an increase, while by increasing L the attenuation can be reduced.

It was not till 1899 that Prof. M. I. Pupin gave a practical solution of the problem of providing telephone lines possessing a low distortion. He proposed the insertion of choke coils in the lines at regular intervals for the purpose of increasing the self-induction of the line. Pupin demonstrated that the expressions for the propagation constant of cables with a uniformly distributed self-induction are still valid when the self-inductions are concentrated at regular intervals, provided the distances of the coils are small compared with the wave-length. He calculated that the ratio of the attenuation of a line with concentrated self-inductions to the attenuation of an equivalent line with uniformly distributed self-inductions was as ${}^1/_2\,\beta_s : \sin {}^1/_2\,\beta_s$, when β_s is the phase displacement of the wave between two consecutive coils. For small values of β_s, i.e. where the distance between two coils is small compared with the wave length, α is roughly equal to α'. If ${}^1/_2\,\beta_s$ is much greater than $\sin {}^1/_2\,\beta_s$, then also α will be much

greater than a'. It is therefore necessary to make the distance between consecutive coils such that also at the highest frequency to be transmitted a sufficient number of coils per wavelength are present.

The first cables equipped with Pupin or loading coils were laid at the beginning of this century. These coils were composed of an annular core made of thin steel wire which was surrounded by a toroidal winding of copper wire. The toroidal form was intentionally selected to keep the external fields of the coil as small as possible, in order to prevent the coils, of which large numbers were accommodated in large iron tanks, from influencing each other.

Since that time the laboratories of the various telephone manufacturers have been studying in great detail the core material for these coils. The result of this work has been not only a marked reduction in the dimensions of the coils, but also a considerable improvement in their characteristics.

Copper and Iron Losses

We shall first study the principal characteristics which must be possessed by loading coils.

The copper and iron losses in loading coils naturally increase the attenuation of the line and it is therefore desirable to keep them small as compared with the natural resistance of the line. The copper losses may be traced back to the ohmic resistance of the winding, which can be kept small by choosing a material for the core with the maximum permeability. These losses can, however, always be reduced by increasing the dimensions of the coil.

The iron losses can be differentiated under three heads: the eddy-current losses, the hysteresis losses and the losses due to magnetic viscosity.

The eddy-current losses are due to the production of eddy currents in the core; they are proportional to the square of the frequency and to B_0^2, if B_0 represents the amplitude of induction in the core. As is well known these losses can be reduced by subdividing the core; this subdivision is continued until the losses at the maximum frequency to be transmitted can be neglected as compared with the losses due to the ohmic resistance.

The hysteresis losses are proportional to the frequency and, for small current amplitudes, also proportional to B_0^3 [1]). The eddy-current and hysteresis losses can be expressed in the form of a loss resistance, multiplied by the square of the current intensity. If we put the induction B_0 proportional to the amplitude of the current, it is found that the resistance representing the eddy-current loss is independent of the current, while the hysteresis-loss resistance increases in proportion to the amplitude of the current.

As shown in another connection [2]), a resistance dependent on the current results in non-linear distortion, so from this point of view it is important to make the hysteresis-loss resistance as small as possible. For this reason the induction B_0 must not be made too high.

Since B_0 is proportional to the permeability of the material, the hysteresis and eddy-current losses limit the permissible permeability. This is in contradiction with the requirements stated above as regards the copper losses, so that a compromise must be achieved.

We have also referred to the losses due to magnetic viscosity. As already indicated the eddy-current loss resistance is proportional to the square of the frequency, while the hysteresis-loss resistance is proportional to the first power of the frequencies and the current. Investigation of the iron losses at different frequencies and currents and resulting extrapolation for zero frequency and zero current demonstrates however that there is still another loss resistance. Jordan [3]) has termed this phenomenon the magnetic after effect of viscosity; it is independent of the current and proportional to the frequency. It is however small compared with the other losses and can therefore be neglected in this analysis.

Stability

When the first loading coils had been in use for a few years it was discovered that the self-induction of many coils had undergone a considerable change. The cause of this was found to be due to an alteration in the permeability of the core material by magnetisation with direct current. This magnetisation was the result of abnormally high currents occasionally induced in the telephone lines by lightning or the power conductors of electric railways, etc. The change in self-induction on magnetisation

[1]) On weak magnetisation with alternating current, the following type of relationship is found between the induction B and the field strength H: $B = \mu H \pm \nu (H^2 - H_0^2)$ where H_0 is the amplitude of the field strength and the algebraical sign is negative or positive according as the field strength decreases or increases. The loss in energy per period is given by the surface F of this curve and is found to be:

$$F = \frac{8}{3} \frac{\nu}{\mu^3} B_0^3 .$$

[2]) Philips techn. Rev. 1, 140, 1936 (in the article dealing with the sound recorder of the Philips-Miller system).

[3]) H. Jordan, E.N.T. 1, 7, 1924.

by passing a direct current of 1 A through the line was taken henceforth as a measure for the stability. In the first loading coils this change might amount to as much as 30 per cent, while in modern loading coils the stability has been raised to less than 1 per cent.

As already stated the cores in the first loading coils were made of thin steel wire. A marked improvement was made in 1916 by the introduction of the compound core.

These cores were made of iron powder which had been compressed under a high pressure with an insulating material. By using powdered iron the path of the lines of force through the core is subdivided; this subdivision thus acts similarly to an air gap, except that in the compound cores this gap is spread uniformly over the whole length of the lines of force, whereby symmetry is retained and the stray field remains small.

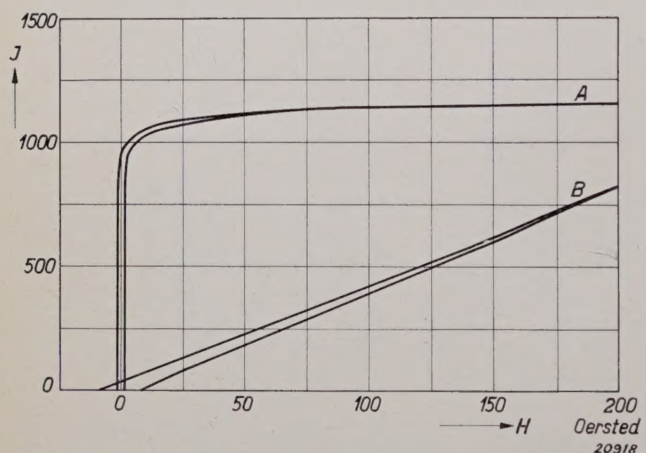

Fig. 2. Magnetisation curves of nickel-iron strip for loading coils.
A) Magnetic field perpendicular to the direction of rolling.
B) Magnetic field parallel to the direction of rolling.

Owing to the air gap the induction at constant field strength is reduced. If *A* in *fig. 2* represents the magnetisation curve of the original material, the curve for the compound core is found to be less steep, roughly as shown by *B*. This second curve has a much greater stability and smaller hysteresis losses.

Since that time progressive improvements have been made on the material used for coil cores. Better characteristics were sought in different directions, e.g. by modifying the shape of the metal particles and in the choice of insulating medium. Efforts were also made to obtain directional orientation of the metal particles by applying a magnetic field to them during the pressing process; but the principal work was directed towards the use of metallic alloys with a high initial permeability and low hysteresis losses. The best known alloys employed for this purpose are the nickel-iron alloys, such as Permalloy which was evolved in America.

Some details are given below of a material for making the cores of loading-coils, which was produced a few years ago in the laboratories of the Philips Works. The development of this material was based on the fact that the remanence must be small and *B* must be proportional to *H*. The magnetising curve had therefore to be of the form shown for the powder material Permalloy (see curve *B* in fig. *2*).

It was well known that certain nickel-iron alloys which had a very high remanence in the normal annealed state exhibited a lower remanence and a suitable hysteresis curve in the hard-rolled condition. A hard-rolled alloy of this type would therefore prove a suitable material for making cores if its necessary properties could be still further enhanced.

To investigate whether this could be done cores were made of a nickel-iron alloy which was rolled down to a strip of 60 microns, then insulated with varnish and finally wounded up to a coil core (see *fig. 3*). To enable the material to be rolled easily it was reheated several times during the rolling process.

It became immediately apparent in the first ex-

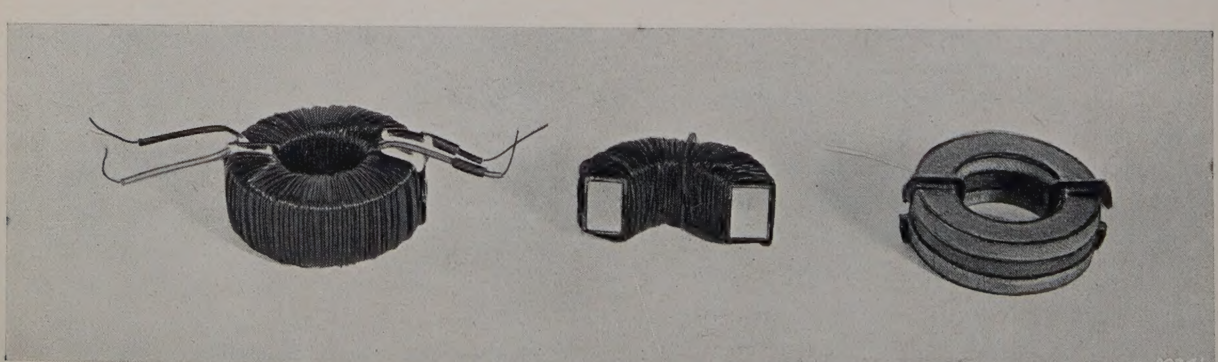

Fig. 3. Loading coil. *a*) Ready for fitting. *b*) Cross-section. *c*) Coil core.

periments made that cores manufactured by this process exhibited marked differences as regards hysteresis losses. These losses were five times greater with several coils as with others. The high hysteresis losses were always accompanied by a high remanence.

After tracking down the causes of these differences, the following manufacturing process was evolved, which furnishes a material with very low hysteresis losses and a satisfactory stability. A nickel-iron strip was rolled down to approx. 0.1 mm and recrystallisation then induced by reheating; the strip was then rolled down to 60 microns and again annealed at a temperature of approx. 400 °C during which stage no recrystallisation takes place.

Each of the four stages of this process has its own specific importance. During first rolling the nickel-iron undergoes marked deformation in the direction of rolling, as a result of which a very characteristic structure is obtained on subsequent recrystallisation: The axes of the crystals, with very low deviation, lie parallel to the length, breadth and depth of the strip.

This pronounced crystal structure causes the appearance of stresses in the material during the subsequent rolling process (reduction from 0.1 mm to 60 microns), the material also becoming magnetically anisotropic. The magnetisation curves of the rolled strip obtained on magnetisation in the direction of rolling and perpendicular to it are observed to be essentially different. The are given by the curves B and A respectively in fig. 2. We have thus obtained a material which on magnetisation in the direction of rolling has very low hysteresis losses.

The fourth stage in manufacture, annealling, is merely carried out for the purpose of reducing the internal stresses, as a result of which the permeability rises without the low hysteresis value in the longitudinal direction increasing too much.

The effect of this annealing process is shown clearly in *fig. 4*, giving the curves for the permea-

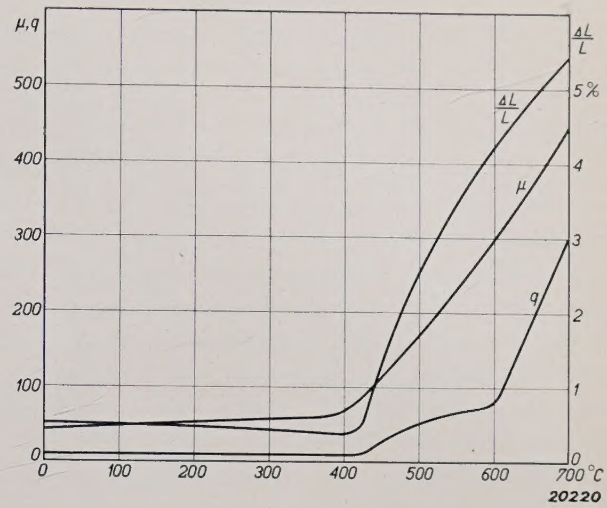

Fig. 4. Permeability μ, hysteresis value q and stability $\Delta L/L$ as a function of the temperature after last re-heating. It is seen that the hysteresis has its lowest initial value up to 400 °C. At this temperature the permeability has already considerably increased, while the stability has reached an optimum at this value.

bility μ, the hysteresis value q [4]) and the stability $\Delta L/L$ as a function of the temperature of annealing.

For the type of coil shown in fig. 3 the following practical values were obtained.

Permeability $\mu = 80$

Hysteresis value $q = h/\sqrt{L} = 7$

Stability $\Delta L/L = 0.5$ per cent.

The volume of the core was 23 cm³ and that of the coil 60 cm³.

[4]) The hysteresis value $q = h/\sqrt{L}$ gives a figure for the hysteresis losses of the coil which is independent of the number of turns and is only determined by the dimensions and the material of the core. Here h is the hysteresis factor, i.e. the increase in the hysteresis loss resistance per henry and mA at 800 cycles/sec.

TELESCOPE MIRRORS

By H. J. MEERKAMP VAN EMBDEN.

Summary. The degree of precision to which the surface of mirrors must conform to the true shape for use in large reflecting telescopes is exceptionally high. Deviations from the true shape occur owing to sag and bending under its own weight and also owing to small temperature changes at the upper and lower surfaces of the glass disc. A process is described here in which the thick disc of glass normally employed is replaced by a chromium-iron casting, one surface of which is coated with a thin glass layer on which the reflecting surface is ground.

The history of astronomy and particularly of astrophysics is very closely related to the evolution of the instruments used for observations in these subjects. Before the invention of the refracting telescope only the paths of the planets could be observed and described; a deeper delving into the structure of the universe could not be essayed. The first refracting telescopes were made about 1580 by Giambettista della Porta in Italy and by Zacharias Jansen (1608) in Holland. The Dutch telescope, which was originally invented as an instrument for use in warfare and offered to Prince Maurits for this purpose, very soon became widely known and was also sold in Paris, Galilei in Padua thus obtaining information of its existence. He realised the importance of the invention and himself built a telescope on the same lines. From this time dates a rapid expansion of knowledge of the structure of universe: The discovery of the satellites of Jupiter, the "mountains of the moon", the starry clusters of the Milky Way, and spots of the sun, etc. By the applications of spectrum analysis and photography in the nineteenth century a more profound knowledge of these phenomena was gained.

Together with the refracting telescope, the reflecting telescope was also undergoing development. Newton (1640—1720) gave the first impetus to its evolution by his discovery that a mirror, contrary to a lens, does not possess chromatic aberration.

In the histories of the refracting and reflecting telescopes we are confronted with an example of the keenest mutual competition in which each instrument in its turn occupied the position of favour and preference. During recent years the reflecting telescope has come more and more to the fore, after a telescope with a mirror of 100″ diameter was put into commission in 1918 at the Mount Wilson Observatory. At the present time an instrument is under construction with a mirror having a diameter of 200″. It should be noted for purposes of comparison that the largest telescope, that at the Yerkes Observatory, is equipped with a lens of 40″ diameter, so that for the largest instruments the reflecting telescope holds unchallenged priority.

Yet both instruments have their own specific fields of application. The refracting telescope is employed in general for visual observations and for astronomical purposes, while the reflecting telescope, particularly those of large dimensions, is the ideal instrument for the observation of objects having a low luminosity as well as for spectrographic and photographic work. The image obtained with the refracting telescope is still sharp at some distance from the optical axis and in this respect gives better representation than the reflecting telescope; the latter is however a better condenser of the feeble light emitted from very distant objects. Moreover, reflecting telescopes are frequently favoured by amateurs since they are easier to make than refracting telescopes giving the same brightness of image.

To eliminate chromatic aberration the objective of a telescope must be composed of at least two lenses, which entails grinding and mutually centering four surfaces on each objective, as against only one surface in a reflecting telescope where chromatic aberration is absent. Furthermore, in the objective of a refracting telescope part of the incident light is reflected at the surface and absorbed by the glass; this absorption is most pronounced with short wavelengths to which photographic plates are most sensitive. The efficiency of the reflecting telescope is therefore the more satisfactory, especially as in the most modern types the surface is coated with aluminium instead of silvered, mainly because an aluminium coating gives a satisfactory reflection of that part of the spectrum required for photographic purposes. Reflection at the silvered surface of a telescope mirror is much reduced if the silver surface tarnishes by exposure to air, so that it must be renovated at regular intervals by replating.

The most important component of the reflecting telescope, the mirror, was originally made of metal.

Socalled "mirror metal", an alloy of 68.3 per cent copper and 31·7 per cent tin, has been known for many years and has proved extremely efficient. One disadvantage was, however, its brittleness and its difficulty to work, making the manufacture of large units impossible. By altering the composition it was indeed found possible to cast larger objects, but only at the expense of the surface, which after a short time lost its polish and no longer gave a good reflection. Owing to the extreme accuracy required of the surface, renovation cannot be resorted to and a metal mirror once having lost its reflecting surface cannot be reconditioned.

Nevertheless mirror metal was the only material available to the famous English builders of telescopes, Herschel, Lord Rosse and Lassell in the 19th century when constructing their large telescopes — up to a diameter of 72″ — with which they made a large number of important discoveries.

It was not until 1857 that Foucault described a new method of preparing a reflecting surface. He made a glass disc with the requisite shape of surface and by chemical means coated this surface with a very thin layer of silver. If the surface becomes dull by contact with the air, the silver was merely dissolved off and a new silver coating was deposited on it, without the shape of the surface being in the least way altered. This method was very successful and is still in general use. In recent years, however, Dr. Strong of Pasadena has evolved a process in which the silver coating is replaced by aluminium, which is deposited on the glass in a high vacuum by volatilisation. On exposure to air the aluminium becomes coated with an extremely thin film of oxide, but is subsequently not further attacked by the atmosphere.

If we examine the causes which limit the observation of extremely distant objects in the universe when using large telescope mirrors, we find that these causes fall naturally into two groups: One group is independent of the instrument used, and the other group is inherent in the instrument.

In the first group we have the lack of homogeneity of the atmosphere and the occurrence of disturbing light, and in the second group inaccuracies in the surface of the mirror and abnormalities due to stresses in the materials used and created in shaping them.

Difficulties Independent of the Instrument

The observation of objects beyond the earth's atmospheric mantle is rendered difficult because the air through which the emitted light reaches the observer is not at rest but in constant motion. If the air were homogeneous, this motion would have no effect; but owing to differences in temperature and humidity this is by no means the case, and the irregular refraction of the light rays during their passage to the instrument frequently prevents reliable observations being made.

In addition there are other disturbances due to the atmosphere surrounding the earth not being wholly transparent, but being permeated with dust and fog particles in suspension. Their presence not only causes diffuse dispersion of part of the emitted light, but has the same effect also on light from other sources, so that a star cannot be seen against a perfectly dark background but only against a background which itself appears to have a certain brightness. The greater the surface of the telescope mirror, the more light from the star under observation will be collected at the focus and the greater will be the contrast against the background.

To restrict the effect of this diffuse-dispersed light, it has been decided to erect the 200″ telescope now in course of construction in America not on Mount Wilson alongside the existing 100″ telescope, which is the largest one in use at the present time, but on Mount Palomas (3300 m) at a distance of 150 km. The reason for this is that the valleys surrounding Mount Wilson have become densely populated during recent years and it has become essential to locate the new observatory at some more distant spot.

Difficulties Inherent in the Instrument

While the difficulties described above are beyond the control of the instrument builder, he must nevertheless give the most careful consideration to the following points since they have a paramount bearing on the efficiency and utility of the instrument. We will therefore discuss these difficult points in order.

The correct theoretical shape for the surface of the mirror is a paraboloid and every deviation from this ideal shape results in a reduction in the quality of the image. The first question which therefore arises is: How far can the actual shape of the surface deviate from the ideal theoretical shape, in other words what tolerance is permissible in the preparation of the surface? The best known rule for this is that given by Lord Rayleigh, according to which the maximum deviation at any point must not exceed $^1/_8$ of the wavelength of visible light or approx. 0.07 μ. It is thus evident to what high degree of accuracy the surface must be worked, since in machining metals a precision

to within several microns already calls for the most exceptional accuracy on the part of the machines used. That the difficulties in making large mirrors become rapidly greater with the size is also apparent, for it is a very different matter to work to this precision with a surface of 28″^{2} (a mirror of 6″ diameter) than with a mirror of 30000″^{2} surface, i.e. of 200″ diameter.

Although this requirement *per se* is already difficult enough to fulfil, it is rendered still more onerous by the fact that a telescope mirror is not a perfectly rigid body, since when the instrument is turned in different directions elastic deformation is set up within it while changes in shape are also produced by temperature gradients. As a result of these deviations a telescope may become quite useless.

Hitherto telescope mirrors have been made of glass, with the lower surface flat and the upper surface ground convex and then silvered. If a plate of this type is supported at three points in the usual way and is then turned out of its horizontal position in following the path of a star a deformation must inevitably occur. In a horizontal position the mirror bends at the centre under its own weight, while when exactly vertical the force of gravity creates a quite different type of deformation. In the case of a massive disc the deformation in the vertical position can be neglected, but this cannot be done when the plate is horizontal and has a diameter exceeding about 8″.

Consider two mirrors made of the same material, then according to investigations by Couder[1]) the sag of the mirror is proportional to R^4/h^2, where R is the radius and h the thickness of the mirror. It is thus possible to keep the deformation small by making the thickness large as compared with the diameter; but difficulties are then encountered in manufacture as well as in erection which limit the advantages to be gained by this means.

With two mirrors of the same dimensions, but of different materials, the sag at the centre was found to be proportional to d/E, where d is the density and E the modulus of elasticity. Thus if we compare glass and bronze, two materials which are commonly used for making mirrors, it is found that E is the same for both materials, viz. approx. $7 \cdot 10^5$ kg per sq cm, while the density of bronze is 8 and that of glass $2^1/_2$, so that in this case glass would be much more suitable than bronze.

In the large telescopes in use at various observatories, the mirror is usually given extra support at different points by means of a complicated system of levers with counterweights, thus eliminating the effect of the dead weight of the mirror. If these mirrors are raised towards the vertical, the opposing pressure applied by the counterweights diminishes.

We shall now turn to another factor which affects the deformation, viz., the variable temperature distribution over the mirror. Already during the manufacture of the mirror this effect becomes apparent, since the grinding media cause the evolution of heat on the worked surface, while the lower side of the mirror remains at a lower temperature. As a result the upper surface expands relative to the lower one, resulting in a deviation from the correct curvature, so that further grinding or measurement must be postponed until the temperature has again become uniform. The opposite state of affairs rules during the employment of the mirror: The surface directed towards the heavens becomes cooled during night observations, while the lower surface protected by a cushion of still air between the back of the mirror and the mount is subject to less cooling. This temperature difference again results in a change in shape, unless provision for a temperature equilibrium is made by thermal conduction of the glass and by radiation. Couder also investigated this phenomenon and found that with equivalent dimensions the deformation occurring is proportional to $a\,d\,c/k$, where:

a is the coefficient of linear expansion,
d the density,
c the specific heat, and
k the thermal conductivity.

To reduce these deformation effects Pyrex glass has been used in place of ordinary glass, the former having a lower coefficient of expansion and a greater thermal conductivity.

	Coefficient of expansion = Relative elongation per °C	Thermal conductivity cal cm^{-1} sec^{-1}
Pyrex glass	$3 \cdot 10^{-6}$	0.012
Ordinary glass	$9 \cdot 10^{-6}$	0.005

With metal mirrors a considerable improvement could be achieved in this respect, since the conductivity of metals is approx. 100 times greater than that of glass.

A third cause of deformation is that temperature differences can occur not only between the upper and lower sides of the mirror but also between the

[1]) A detailed investigation of this point is described by A. Couder in Bull. Astron. VII, 1931.

Fig. 1. Rear side of the 12″ mirror. The casting by which the mirror is later secured in the telescope can be clearly seen. During surface working which is done by hand a wood ring is attached to the casting to provide a grip.

rim and the centre. As a result of this the zone at the rim may become so highly deformed that the sole remedy possible is to place a diaphragm in front of the mirror, which naturally reduces its useful reflecting surface. In this respect again a metal mirror would be less sensitive.

Mirrors in the past have been made exclusively in the form of massive discs, except the 200″ mirror of Pyrex glass now in course of manufacture, which is made up of a plate ribbed on the lower side. A ribbed construction of this type offers various advantages, but could not be hitherto employed owing to the great difficulty of casting complicated shapes of glass.

Fig. 2. Casting for a 12″ concave mirror (focal length 80″). On affixing the glass, part has run over the edge. Shaping is done by polishing two glass discs one against the other, using a suitable lubricant (carborundum, alundum or rouge).

The casting of metals is much simpler, although by using metals the important disadvantage already referred to remains, viz., that the surface of the mirror is difficult to work and rapidly deteriorates.

A way to overcome the difficulty has been investigated at this Laboratory for some time past; the new method of manufacture evolved is based on a combination of the desirable properties of glass and metal, viz., the use of a metal mirror which on the upper side is coated with a very thin skin of glass on which the mirror surface is ground.

The metal used is a special chromium-iron alloy whose coefficient of expansion is the same as that of glass and to which the glass can very tenaciously

Fig. 3. Rear side of the 35″ mirror. The supporting framework provides the necessary stiffening for the thin upper surface on which the glass is fused.

adhere. This alloy has found extensive use in vacuum-tight metal-to-glass unions, which form an important component in the larger types of rectifying valve, in transmitting valves and X-ray tubes.

The manufacture of castings from chromium-iron is not much more difficult than from steel and is much simpler than from glass.

Any shape can be cast and the strengthening ribs can be made as thin and as high as required for obtaining the requisite strength, at the same time realising a low weight. Eyes and lugs can also be readily cast on, which can be later machined and threaded to facilitate the fixing of the mirror in its support.

Fig. 4. Chromium-iron casting of 35″ diameter, covered on the front with glass to a thickness of 10 mm (shaded). The glass is later ground completely smooth, after which the surface is silvered.

The casting is readily relieved of internal stresses by reheating, while for the same end glass mirrors must usually be allowed to cool for several months under the most carefully controlled conditions.

The chromium-iron casting is first machined on the rear side and turned flat in a lathe so that the mirror will later lie quite flat when mounted in the polishing machine. The workpiece is then reversed and the top surface which is later covered with glass is then machined. In this operation the surface is roughly shaped to conform with the final surface contour of the mirror.

This is followed by the application of the glass coating. A glass plate is laid on the casting and the assembly then heated in a furnace to above the softening point of the glass. The glass melts and forms a bond with the metal surface below it; the fused glass must not be allowed to get too fluid so that with a concave mirror the whole of the glass collects at the centre. If this operation is correctly performed the glass coating forms a layer of uniform thickness over the whole surface and can therefore be maintained very thin. Little has then to be removed in the subsequent machining process, although the principal advantage is that the thin glass layer can be cooled very rapidly without the production of internal stresses. Cooling takes as many hours as months were required in the past. It is also possible to sort out the glass plates at the outset and reject all those with any suspicion of air bubbles, inclusions or other defects.

In this way the advantages of metal and glass can be combined, viz., the easy machinability, good conductivity and ease in fixing of metal and the excellent surface and every facility for silvering or aluminium coating offered by glass.

A concave mirror 12″ in diameter *(figs. 1 and 2)* manufactured by this process was placed at the disposal of a number of amateur astronomers at Eindhoven, who are now grinding it down to give a focal length of 80″. This mirror will be used in a telescope being built for its reception.

A plane mirror with a diameter of 36″ *(figs. 3 and 4)* was supplied to the Californian Institute of Technology. It is now being ground and is to be used as a mirror in a coelostat, i.e. an instrument which at a plane mirror rotated by clockwork reflects the light emitted from a star or other heavenly body so that the measuring instruments used can be kept stationary.

When using such coelostats for solar observations, a glass mirror introduces considerable difficulties owing to the marked differences in temperature which occur during the measuring period, while metal mirrors have the disadvantage that the surface gradually deteriorates and the power of reflection becomes considerably reduced.

The advantages of the new process thus become strikingly apparent in this application.

ELECTRICAL FILTERS V

Vacation course, held at Delft, April, 1936,

By BALTH. VAN DER POL and TH. J. WEIJERS.

Summary. In this article the transient phenomena in non-dissipative low-pass filters are analysed. With the aid of Heaviside's operational calculus the cut-in current of the n-th section of an infinitely long filter composed of a number of equivalent sections of basic type is calculated. By repeated subdivision of the filter sections the continuous cable is obtained at the limit with uniformly-distributed inductance and capacity. On passing to the limit, it is found that the impressed impulse is propagated without distortion and at a specific velocity through a non-dissipative cable. It is indicated in the last section how the transient phenomena in high-pass filters can be deduced from those derived for low-pass filters.

In the previous articles of this series the behaviour of filters when sinusoidal e.m.f. is impressed on them was investigated. From the results obtained the behaviour of the filter on the application of a non-sinusoidal but still periodically-varying voltage could also be deduced. This voltage can be expanded as a Fourier series, each term of which can be dealt with independently and the results then added by the principle of superposition (p. 242).

Conditions are, however, different where the voltage is not a periodic function, and in this case it is not possible to expand it as a Fourier series. An example of a non-periodic voltage sequence is the phenomenon obtained when closing a circuit; in this case transient phenomena are encountered.

These phenomena will be analysed in detail below. The simplest case is the sudden impression of a direct voltage which will be assumed, for the sake of simplicity, to be unity, and to remain constant after the circuit is closed, on a filter carrying neither current nor voltage. *Fig. 1* gives this voltage as a function of the time: For $t < 0$, $V = 0$ and for $t > 0$, $V = 1$.

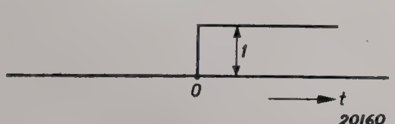

Fig. 1. The Heaviside unit function.

This function will be termed the unit function, in accordance with Heaviside, and will be represented by the symbol [1]. In this article we shall limit discussion to low and high-pass filters of fundamental form when this unit voltage-time function is impressed on them.

We shall employ the operational or symbolic calculus, which is based on the following principle: If $i(t)$ is an arbitrary function of the time, a function with another variable p can be obtained by means of the following expression (Carson's integral):

$$p \int_0^\infty e^{-pt}\, i(t)\, dt = f(p) \quad . \quad . \quad . \quad . \quad (1)$$

The symbolic form of equation (1) is:

$$i(t) \doteqdot f(p) \quad . \quad . \quad . \quad . \quad . \quad . \quad . \quad . \quad . \quad (2)$$

For each given function $i(t)$, $f(p)$ is defined by (1) and vice versa. $f(p)$ is termed the operational representation of $i(t)$. If $i(t)$ represents a current and if at time $t = 0$ the current and all time derivatives are equal to zero, then it follows that:

$$\left.\begin{array}{l} \dfrac{d}{dt}\, i(t) \doteqdot p\, f(p) \;; \\ \dfrac{d^2}{dt^2}\, i(t) \doteqdot p^2\, f(p) \;; \\ \quad\vdots \\ \dfrac{d^n}{dt^n}\, i(t) \doteqdot p^n\, f(p) \;. \end{array}\right\} \quad . \quad . \quad . \quad . \quad (3)$$

Differentiation with respect to t therefore corresponds to a multiplication by p (and not by $j\,\omega$, as in the complex method). Similarly integration corresponds to a multiplication by $1/p$. We get by calculation with the aid of equation (1):

$$\int_0^t i(t)\, dt \doteqdot \frac{1}{p}\, f(p) \quad . \quad . \quad . \quad . \quad . \quad . \quad (4)$$

We thus obtain a transformation from the known complex method to the operational calculus, if $j\,\omega$ is replaced by p.

The operational representation of the unit function [1], which is now under consideration, is according to equation (1):

$$[1] \doteq p \int_0^\infty e^{-pt}\,[1]\,dt = p \int_0^\infty e^{-pt} \cdot 1 \cdot dt = 1\,,$$

$$[1] \doteq 1 \quad . \; . \; . \; . \; . \; . \; . \; (5)$$

A potential impressed at the time $t = 0$ which subsequently remains constant is thus represented in the operational calulues by a constant which is equal to the absolute value of this potential.

Low-Pass Filter of Basic Type on the Application of the Heaviside Unit Function

Consider a low-pass filter composed of an infinite number of T-sections of basic type *(fig. 2)*, or what is the same thing as regards the currents and voltages in the filter, of a finite number of sections which are terminated by the image impedance.

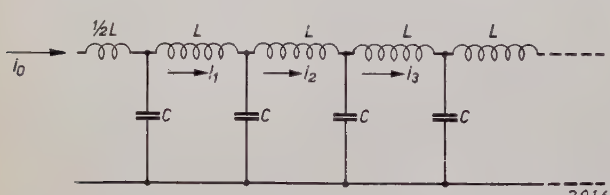

Fig. 2. Low-pass filter composed of an infinite number of T sections of basic type.

We shall discuss this filter in the first place as again having a sinusoidal e.m.f. impressed on it, using the complex method of representation $E_0 e^{j\omega t}$. We shall here make use of the formulae for low-pass filters which were derived earlier [1]) and which are collected together in a comprehensive table on p. 305 of this Review. For the image impedance Z_T', i.e. here the impedance between the primary terminals, we have:

$$Z_T' = R\sqrt{1-x^2} = \sqrt{\frac{L}{C}}\sqrt{1-\frac{\omega^2}{\omega_1^2}} \quad . \quad (6)$$

and the propagation constant T of a single section is given by the expression:

$$e^{-T} = \frac{\sqrt{1-x^2}-jx}{\sqrt{1-x^2}+jx} = \left(\sqrt{1-\frac{\omega^2}{\omega_1^2}}-j\frac{\omega}{\omega_1}\right)^2 \quad . \quad (7)$$

Equations (6) and (7) give Z_T' and T as functions of the angular frequency. ω_1 is the angular frequency at the boundary of the transmission band. The secondary current of the n-th section is i_n, i.e. the primary current of the n-th section (= the secondary current of the $(n-1)$th section) is i_{n-1}.

[1]) Philips techn. Rev. 1, 298, 1936.

The primary current of the first section is thus i_0. If now the voltage between the primary terminals of the filter is $E_0 e^{j\omega t}$, we have:

$$i_0 = \frac{E_0 e^{j\omega t}}{Z_T'} \quad . \; . \; . \; . \; . \; . \; (9)$$

$$i_n = \frac{E_0 e^{j\omega t}}{Z_T'}\, e^{-nT} = \frac{E_0\, e^{j\omega t}}{\sqrt{\frac{L}{C}}\sqrt{1-\frac{\omega^2}{\omega_1^2}}}\left(\sqrt{1-\frac{\omega^2}{\omega_1^2}}-j\frac{\omega}{\omega_1}\right)^{2n} \quad . \; . \quad (10)$$

What does i_n become if no sinusoidal voltage is impressed across the primary terminals of the filter, but a unit potential function [1]? We obtain the operational representation of this current $i_n(t)$ by substituting in equation (10) p for $j\omega$ and 1 for $E_0 e^{j\omega t}$, thus:

$$i_n(t) \doteq \sqrt{\frac{C}{L}}\frac{1}{\sqrt{1+\frac{p^2}{\omega_1^2}}}\left(\sqrt{1+\frac{p^2}{\omega_1^2}}-\frac{p}{\omega_1}\right)^{2n} \quad . \quad (11)$$

In order to determine to which time function this operational expression (11) corresponds, i.e. how the current in the n-th branch depends on the time, expression (11) is substituted in the integral equation (1). We have therefore to solve the integral equation:

$$p\int_0^\infty e^{-pt}\, i_n(t)dt = \sqrt{\frac{C}{L}}\frac{1}{\sqrt{1+\frac{p^2}{\omega_1^2}}}\left(\sqrt{1+\frac{p^2}{\omega_1^2}}-\frac{p}{\omega_1}\right)^{2n} \qquad (12)$$

and to answer the question: What function $i_n(t)$ on integration gives this result?

The operational representation of a large number of functions is known; the right hand side of equation (11) belongs to the group of known expressions:

$$\int_0^{\omega_1 t} J_{2n}(x)\,dx \doteq \frac{1}{\sqrt{1+\frac{p^2}{\omega_1^2}}}\left(\sqrt{1+\frac{p^2}{\omega_1^2}}-\frac{p}{\omega_2}\right)^{2n} . \quad (13)$$

It thus follows from (11) and (13):

$$i_n(t) = \sqrt{\frac{C}{L}}\int_0^{\omega_1 t} J_{2n}(x)\,dx\,, \quad . \; . \; . \quad (14)$$

where $J_{2n}(x)$ is the Bessel function of the $2n$-th order with the argument x.

Equation (14) thus gives the current obtaining behind the n-th section of a low-pass filter composed of T-sections of basic type, if at the input of the filter at time $t = 0$ a direct voltage of unit

value is suddenly applied, and the filter before $t = 0$ carried neither current nor voltage.

Fig. 3 shows the current in the self-induction of the fourth section, i.e.

$$i_4(t) = \sqrt{\frac{C}{L}} \int_0^{\omega_1 t} J_8(x)\, dx$$

as a function of $\omega_1 t$. It is seen that the current $i_n(t)$ remains very small up to time $t = 2\, n/\omega_1$; it then commences to be built up and finally fluctuates about $\sqrt{C/L}$ with gradually diminishing amplitude. This is the analogue of the finite time of transmission of a signal as found in the case of cables. In our case the current has passed through n sections in the time $t = 2\, n/\omega_1$, so that per second $n/t = {}^1/_2\, \omega_1$ sections are traversed. The velocity of propagation is therefore ${}^1/_2\, \omega_1 = 1/\sqrt{LC}$ sections per second.

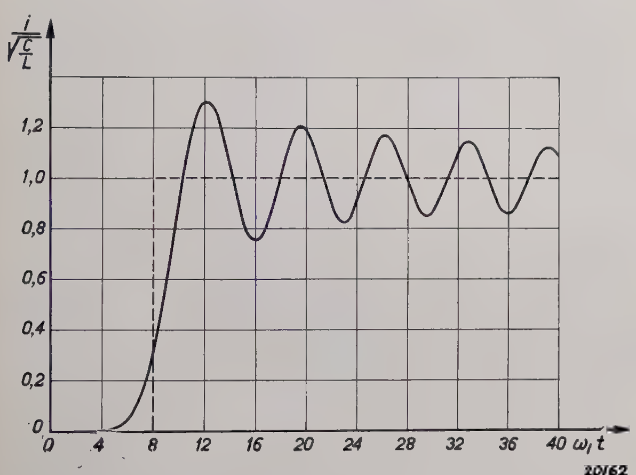

Fig. 3. The current in the self-induction of the fourth section of a low-pass filter composed of an infinite number of sections of basic type (or a finite number of sections terminated by the image impedance), when unit potential [1] is impressed at the input of the filter at $t = 0$. This current is represented by

$$i_4(t) = \sqrt{\frac{C}{L}} \int_0^{\omega_1 t} J_8(x)\, dx,$$

where ω_1 is the limiting frequency of the filter. The broken line indicates the current at the same point when the filter is transformed into a continuous cable by infinite subdivision of the filter sections.

Transition from a Low-Pass Filter to a Continuous Cable

The filter discussed in the previous section consisted of a group of equivalent T-sections connected in series. If each T-section is replaced by a series-connected group of other T-sections, with self-inductions and capacities an m-th part of the original filter, the total self-induction and total capacity will both remain unchanged. Since, furthermore, the limiting frequency of the filter $\omega_1 = 2/\sqrt{LC}$ is determined by the self-induction and the capacity per section, it will be multiplied by m on subdivision of the section. If this demultiplication is continued ad infinitum, we get the continuous cable at the limit $m \to \infty$ viz., a uniformly distributed self-induction in series and uniformly-distributed capacity in parallel throughout the cable. As m has been taken to infinity, the limiting frequency of the cable will be infinite. A cable devoid of resistance (i.e., non-dissipative) will transmit all frequencies without attenuation. The impedance of the cable is the limiting value of

$$Z_T' = \sqrt{\frac{L}{C}} \sqrt{1 - \frac{\omega^2}{\omega_1^2}}$$

i.e.

$$Z_T' = \sqrt{L/C}.$$

The behaviour of the cable on the application of the unit function [1] can be derived from the behaviour of the filter already investigated and from which we have derived the cable as the limiting case.

Consider the point A which in the original filter was located at the end of the n-th section, and assume that the current at that point is $i_A(t)$. If each section is subdivided into m sections, then for each new section the self-induction will be L/m and the capacity C/m, so that the limiting frequency of the filter is no longer $2/\sqrt{LC}$, but:

$$\omega_1 = \frac{2\, m}{\sqrt{LC}} \quad \ldots\ldots \quad (15)$$

The current at the point A now follows from equation (11):

$$i_A(t) = i_{mn}(t) \doteqdot \sqrt{\frac{C}{L}} \frac{\left(\sqrt{1 + \frac{p^2\, LC}{4m^2}} - \frac{p\sqrt{LC}}{2m}\right)^{2mn}}{\sqrt{1 + \frac{p^2\, LC}{4m^2}}} . \quad (16)$$

If subdivision of the sections is continued to infinity, i.e. $m = \infty$, the filter passes over into the continuous cable. The total self-induction between the input of the filter and the point A remains $n\, L$, and the total capacity $n\, C$. If l is the length of the cable between the input and the point A, the self-induction per unit of length is $\overline{L} = nL/l$ and the capacity per unit of length $\overline{C} = n\, C/l$. For the sake of abbreviation insert $1/\sqrt{\overline{L}\, \overline{C}} = c$ and we get:

$$LC = \frac{l^2}{n^2} \overline{L}\, \overline{C} = \frac{l^2}{n^2 c^2} \quad \ldots \quad (17)$$

Substitution in equation (16) then gives:

$$i_A(t) \doteqdot \sqrt{\frac{C}{L}} \frac{\left(\sqrt{1+\frac{p^2l^2}{4m^2n^2c^2}} - \frac{pl}{2mnc}\right)^{2mn}}{\sqrt{1+\frac{p^2l^2}{4m^2n^2c^2}}} \quad . \quad (18)$$

If m in this expression is taken to infinity, we get the limiting case of the continuous cable, thus:

$$i_A(t) \doteqdot \lim_{m\to\infty} \sqrt{\frac{C}{L}} \frac{\left(\sqrt{1+\frac{p^2l^2}{4m^2n^2c^2}} - \frac{pl}{2mnc}\right)^{2mn}}{\sqrt{1+\frac{p^2l^2}{4m^2n^2c^2}}} =$$

$$= \lim_{m\to\infty} \sqrt{\frac{C}{L}} \cdot 1 \cdot \left(1 - \frac{pl}{2mnc}\right)^{2mn} =$$

$$= \sqrt{\frac{C}{L}} \cdot e^{-pl/c} \quad . \quad . \quad . \quad . \quad . \quad . \quad . \quad . \quad . \quad . \quad . \quad . \quad (19)$$

Since the impedance of the cable at every point is $\sqrt{L/C}$, the operational representation of the voltage at the point A is:

$$e_A(t) \doteqdot e^{-pl/c} \quad . \quad . \quad . \quad . \quad . \quad . \quad (20)$$

This is, the operational representation of the unit function [1], which however does not operate at $t = 0$, but at $t = l/c$, as demonstrated in *fig. 4*.

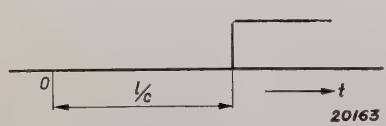

Fig. 4. Current through a continuous cable at a distance l, when the potential at the input is represented by the Heaviside unit function.

Thus the unit potential [1], which was impressed on the cable at the input end, arrives at the point A free from distortion as a unit potential after the elapse of the time $t = l/c$. Hence on the transition from a low-pass filter to a continuous cable a distortionless propagation is obtained with a time of transmission of l/c, in accordance with the elementary theory of electric cables. Propagation has in fact become free from distortion because the limiting frequency in the transmission band has been displaced to infinity. For a non-dissipative cable located in an area without dielectric losses and with a dielectric constant $\varepsilon = 1$ the self-induction and capacity assume such values that the velocity of propagation c is equal to the velocity of light. If $\varepsilon > 1$, c will be smaller than the velocity of light.

Transient Phenomena with High-Pass Filters of Fundamental Form

Hitherto we have limited discussion to transient phenomena with low-pass filters; the results obtained can be applied to high-pass filters with the aid of a mathematical transformation by which the transient phenomena in a second network can be calculated when those in the first network are known. A necessary condition before this can be done is that the second network must be a frequency-reciprocal of the first network, i.e. it must possess self-inductions at those points where the first network has capacities, and capacities at those points where self-inductions are located in the first network, while the resistances in the two networks must be the same. The values of C^*, L^* and R^* of the second network must be related to the L, C and R values of the first network according to the following expressions:

$$\frac{1}{\omega_1 C^*} = \omega_1 L \ ,$$

$$\frac{1}{\omega_1 L^*} = \omega_1 C \ ,$$

$$R^* = R \ ,$$

where ω_1 is an arbitrary angular frequency in radians. If ω_1 is taken equal to the limiting frequency of the low-pass filter, the latter will pass on applying the above-mentioned mathematical transformation into a high-pass filter with the same limiting frequency and it becomes possible to deduce from expressions derived on highly generalised assumptions [2]) the transient phenomena in high-pass filters in a closed form, directly from the known expressions for low-pass filters as demonstrated above.

Since the high-frequency components of the voltage impulse applied to the first section in this case allow current to flow instantaneously through all series-connected capacities, the retardation found with low-pass filters is absent here, and the currents in all circuits exhibit a discontinuous front, which to some extent complicates mathematical representation. We shall not consider this point in greater detail.

[2]) Balth. van der Pol, Physica 1, 521, 1934.

GAS-FILLED TRIODES

By H. G. BOUMEESTER and M. J. DRUYVESTEYN.

Summary. In this article a description is given of a gas-filled triode, which contains in addition to a cathode, a grid and an anode a cathanode. The manner in which it works and the possibilities of its application are dealt with.

To obtain a specific amplification with the smallest number of amplifying valves, valves must be used in which a definite variation in the grid voltage

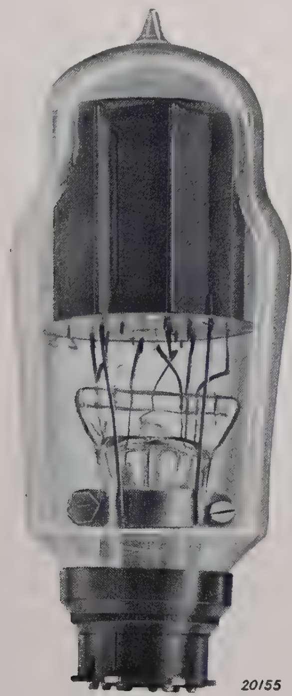

Fig. 1. The gas-filled triode.

produces the greatest possible change in the anode current. In receiving valves of normal ratings the ratio between these two variations, the socalled slope or gradient, is rarely greater than 10 milliamps per volt. Yet if triodes of standard ratings are filled with a small quantity of gas [1]) a slope of 30 milliamps per volt and even more can be realised. In spite of this desirable result there are, however, two important objections against the use of a valve of this type, viz., its marked noise and the fact that the steep slope is maintained only at low frequencies; at higher frequencies (roughly above 10^6 cycles) the slope drops to a much lower value. The relationship between the slope and the frequency is evident when it is remembered that the occurrence of a high slope when using a gas filling is due to ionisation by electrons in the vicinity of the anode; the resultant positive ions possess only a low velocity and thus remove from the space charge a much greater number of electrons, so that the anode current increases considerably. It is just this slow displacement of the positive ions (a result of their great mass) which is responsible for the reduced gradient at higher frequencies.

Some time ago [2]) a valve filled with mercury vapour was described which could be used as triode and which did not possess the above-mentioned disadvantages of the gas-filled triode; in this valve a greater slope was moreover achieved in a somewhat different manner. The general appearance of the valve may be gathered from *fig. 1*, while *fig. 2* shows a section through the Philips type of this valve. *K* is an indirectly-heated cathode. At a distance of 10 mm from the cathode is a rectangular grid (*K A*) made of gauze. It is seen from the longitudinal section that the upper and lower sides of the grid are covered by mica plates *m*. Immediately behind the first gauze there is a second gauze at

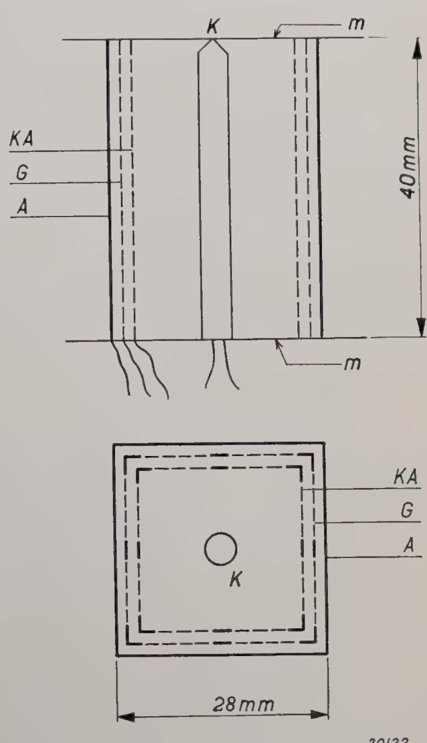

Fig. 2. Section through the gas-filled triode. *K* cathode; *KA* cathanode; *G* grid; *A* anode and *m* mica plates for limiting the discharge.

[1]) Gas-filled valves were used already 20 years ago.

[2]) J. R. Nelson and J. D. le Van, Q.S.T. June 1935, p. 23.

a distance of 1 to 1.5 mm, and directly behind the latter a plate bent at right angles which serves as the anode. The valve bulb contains a drop of mercury so that an atmosphere of mercury vapour is present between the electrodes. The valve functions on the following lines: Between the cathode and the first gauze an arc discharge is produced for which this gauze acts as anode. In the arc a large number of positive ions are formed which dilute the space charge of electrons, so that the running voltage of the arc (i.e. the voltage between cathode and anode) is low, for example 10 volts. Electrons pass through this gauze-like electrode and are attracted to the plate by the second gauze. The plate thus performs the same function as the anode in a vacuum valve, while the second gauze is fully comparable to the grid of a vacuum valve. The first gauze may be compared on the one hand to the cathode of a vacuum valve, and since on the other hand it constitutes the anode of the arc discharge it is termed the "cathanode".

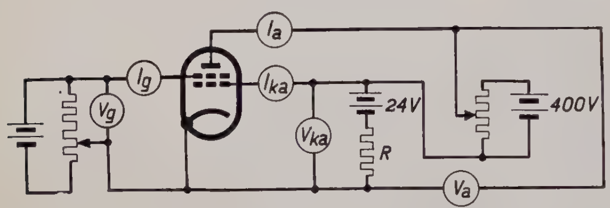

Fig. 3. Circuit for plotting the characteristics. V_a anode voltage, V_{ka} voltage at the cathanode, V_g grid potential, i_g grid current, i_{ka} cathanode current, i_a anode current and R resistance for stabilising the arc discharge.

To measure the characteristics of this valve the circuit shown in *fig. 3* is employed. The arc current, which is e.g. 500 mA, is furnished by a 24-volt battery through a resistance R. The grid and anode voltages are varied by means of potentiometers and the usual characteristics then plotted. The arc current flowing to the cathode is not altered during this measurement, but only that part of this current which flows from either the cathanode or the anode. *Figs. 4* and *5* reproduce a number of characteristics in which the anode current i_a is plotted as a function of the anode volts V_a and the grid voltage V_g respectively. In the example illustrated in the graphs the slope was 27 mA per volt, and the internal resistance 1900 ohms, so that the amplification factor was 51. It is seen that the slope increases with the arc current, while the amplification factor meanwhile changes very little.

The properties of this valve may be explained by regarding the cathanode as a cathode, the action of the valve then being identical to that of a vacuum triode [3]). Since the surface of the cathode is very large and the grid is located close to the cathode, the steep slope is readily accounted

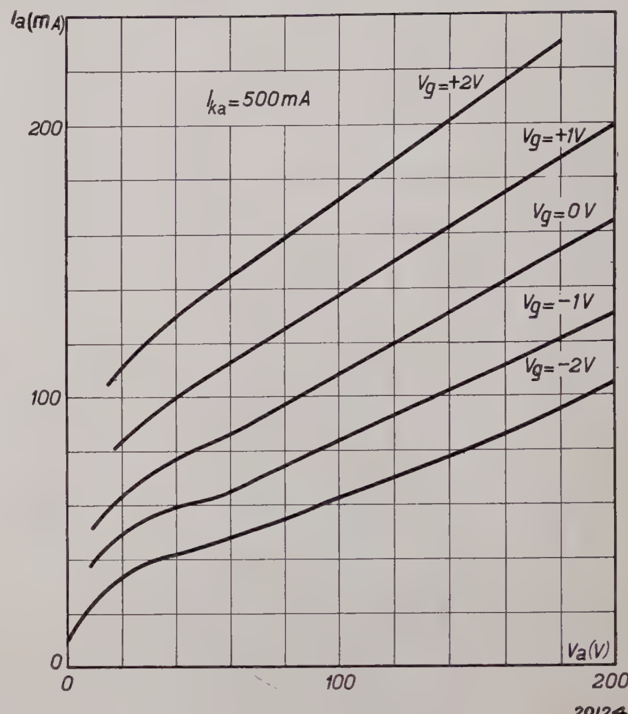

Fig. 4. Characteristics of the anode current i_a as a function of the anode volts V_a for different values of the grid potential V_g. The cathanode current i_{ka} is here 500 mA.

for. The number of positive ions formed between the grid and the anode is small and is not a measure of the slope. As on varying the grid voltage the anode current is also altered but not the arc current, while at the same time the number of positive ions formed between the cathode and the cathanode remains constant, it would be expected that the slope is not related to the frequency, provided the latter does not assume such high values that the time of transit of the electrons has to be taken into consideration. In fact this valve may be quite readily used as an oscillator at a wavelength of, for example, 200 m. The other disadvantage of gas-filled valves mentioned at the outset, viz., the pronounced noise, is also absent in this valve.

---

[3]) A fundamental difference between this virtual cathode and the normal oxide cathode of a vacuum valve is that the mean velocity of emission of the electrons in the second case is only about 0.1 volt as against several volts with the cathanode. It is desirable for the velocity of emission of the electrons at the cathanode to be as low as possible, since the slope increases as the velocity of emission diminishes. This velocity can be reduced by raising the gas pressure as well as by increasing the arc current; the form of the discharge space can also be made more efficient than shown in fig. 2. If, for instance, the anode is enclosed by two grids and the discharge is produced in the outer space where also the cathode must be situated, the discharge space is enlarged and the velocity of the electrons at the cathanode is reduced.

On comparing this valve with vacuum valves it is found that in spite of the absence of the disadvantages referred to above its general application

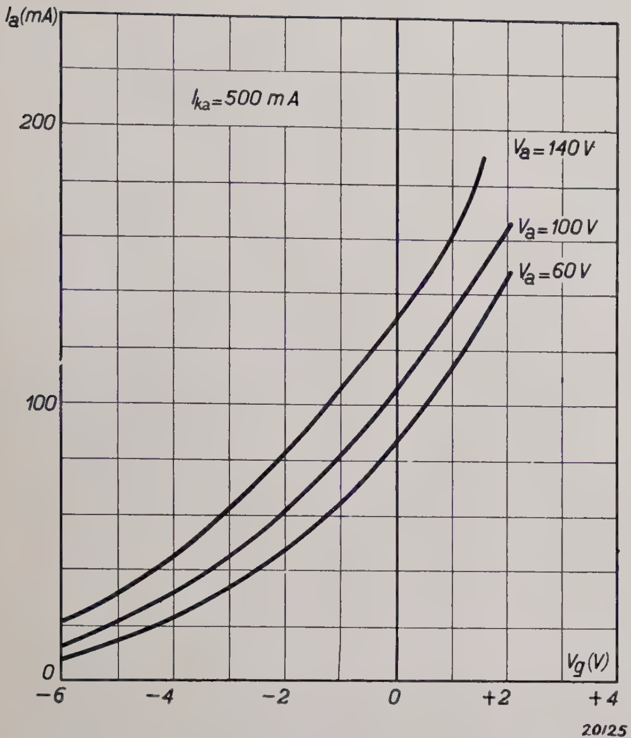

Fig. 5. Characteristics of the anode current i_a as a function of the grid volts V_g for different values of the anode voltage V_a. The cathanode current i_{ka} is here 500 mA.

is nevertheless restricted by several properties in which it differs from those of the vacuum valves. The principal divergent properties are:

1) The cathanode current introduces an additional complication, especially as it is fairly high, e.g. 500 mA, and must be kept constant to a high degree.
2) The grid currents are high, being for instance several mA [4]).
3) The grid-anode capacity is high, since the distance between the electrodes is small, this small interval being indeed necessary in order to limit the ionisation. By introducing a screen grid between these electrodes the capacity can however be considerably reduced.
4) As the pressure of the mercury is governed by the temperature, the characteristics usually vary with fluctuations in the room temperature or when the valve is cooled by a current of air [5]).
5) The i_a-V_g characteristic has a fairly pronounced curvature.

Since these properties are on the whole inherent in the valve described, they restrict considerably the possible use of the valve. It is evident that these properties will prove more undesirable in some applications than in others.

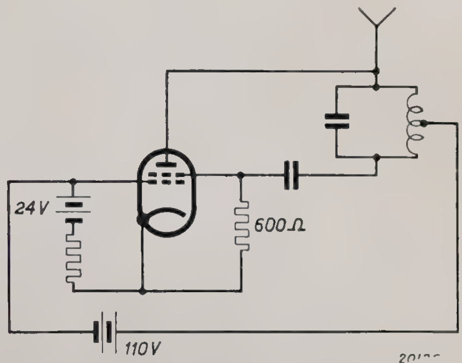

Fig. 6. Circuit for a gas-filled triode used as oscillator in a one-valve transmitter for operating on an anode voltage of 110 V. The cathanode current is furnished by a 24-volt battery.

This valve can be used with marked satisfaction as an oscillator in one-valve transmitters, the pronounced slope permitting the operation of a transmitter of the type shown in *fig. 6* from a 110-volts supply. The anode consumption is here 12 watts, the cathanode current 400 milliamps, and the high-frequency energy 6 watts at a wave-length of 670 m.

[4]) While with a negative grid bias (with reference to the cathode) a current of positive ions flows to the grid which hardly varies with the grid potential, a current of electrons which will vary with the grid potential will flow to the grid when the bias is positive.

[5]) This difficulty could be overcome by using an unsaturated mercury vapour instead of saturated one, or by filling the valve with a rare gas at a low pressure. In the latter case the slope is, however, smaller than when using mercury vapour.

THE DAMPING OF MECHANICAL VIBRATIONS

By A. CRAMWINCKEL, C. J. DIPPEL and G. HELLER.

Summary. Two factors: friction and the decay of the restoring stresses determine the properties of damping agents. In the present article an investigation is made as to how the damping properties depend on the frequency taking into consideration the above two factors. Two groups of damping agents can be distinguished which exhibit fundamentally different behaviours towards vibrations. In the first group, the damping depends mainly on the decay of the restoring stress, and in the second it is due mainly to internal friction. A damping agent of the second group is described, which is suitable for damping the resonances of vibrating mechanical systems.

In the construction of vibrating mechanical systems (for instance for acoustic purposes) it is frequently necessary to damp the undesirable natural vibrations without excessively reducing the sensitivity of the system. In many cases suitable damping can be obtained with air or, where a more powerful action is required, with oil or other fluid. But in many apparatus these forms of damping are not desirable or cannot be realised in practice; it becomes necessary to employ solid damping agents.

Since the damping of vibrations plays an important part in modern engineering, some of the more important aspects of damping agents will be discussed below. We shall first discuss the principal causes producing the damping of vibrations, taking as an example a rectilinear vibration of a point mass under the action of elastic and damping forces. This will be followed by the analysis of a specific technical problem.

Friction and Decay of Restoring Forces as Damping Causes

Two causes of damping will be considered below [1]). The first, friction, is a general phenomenon well known in mechanics. It can be represented by a force which, contrary to elastic forces, always acts in a direction opposite to that of the motion affected and at the same time increases with the velocity. In the simplest case (liquid friction) this force is proportional to the velocity:

$$\text{Force of friction} = -a v = -a \frac{d x}{d t} \quad (1)$$

where x is the distance traversed and a is the coefficient of friction.

There is also a second factor causing the damping of vibrations. If a material, such as ebonite, is allowed to remain for a long time in an elastically deformed state, it will be found that on being released it does not return either at all or wholly to its initial state of equilibrium. The reason for this is that the forces of restitution do not correspond to perfect elasticity, but gradually decay with the lapse of time owing to molecular rearrangements. If with such a material the external forces impressed on it are kept constant, the material will begin to flow in such a way that a reduction of the elastic forces results. If the time of decay τ is introduced [2]), we have the differential law:

$$dK = -c\, d x - K \frac{dt}{\tau} \quad . \; . \; . \; . \; . \quad (2)$$

This law states that the force of restitution with a sufficiently rapid vibration is proportional to the elongation ($K = -c\,x$). If the system is arrested after deflection a decay of the forces will, however, take place with a lapse of time according to the law:

$$\frac{dK}{K} = -\frac{dt}{\tau}.$$

It may be readily seen that this phenomenon also results in a damping of the vibrations. If, for instance, we represent the velocity v by an electric current i and the force K by a voltage V, then the conditions of damping resulting for a point mass are analogous to the damping of an oscillating circuit by a resistance r in series and a second resistance R in parallel to the condenser (see *fig. 1*). It is thus evident that this electrical problem satisfies exactly the same differential equations as the mechanical model, if the circuit elements are so chosen that:

[1]) A detailed discussion of these questions is to be found in J. M. Burgers, Ned. T. Natuurk. 1, 209, 1934; First Report on Viscosity and Plasticity, Proc. Roy. Ac. Sc. A'dam, Physics I., Vol. XV, No. 3.

[2]) The assumption of a time of decay τ independent of the restoring forces, as in the case of our model, signifies that the material already begins to flow at the lowest applied force. In practice, with flow phenomena one is mostly dealing with materials which only commence to flow appreciably above a specific force, the socalled yield point.

$$C = 1/c$$
$$L = m$$
$$r = a$$
$$R \cdot C = \tau$$

It is well known that both the series resistance r and the shunt resistance R produce a damping of

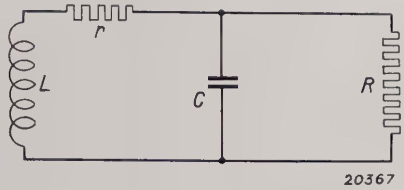

Fig. 1. Substitution circuit for a mechanical vibration with friction and decay of restoring forces. In place of the coefficient of friction a we have the resistance r, and in place of the time of decay τ of the forces of restitution the time of discharge RC of the condenser.

the oscillations. Thus in our mechanical model a damping is similarly produced, both as a result of friction and of the decay of the restoring forces.

Behaviour of Damping Agents with respect to Forced Vibrations

The behaviour of damping agents has a much greater practical importance with respect to forced vibrations — the arresting of vibrating mechanical systems — than with regard to free vibrations. The necessary calculations can be readily carried out by introducing, in addition to the internal forces, which are the same as those for free vibrations, also an external force $k \sin \omega t$.

The following expression is obtained for the absolute value of the amplitude A of vibration:

$$A = \frac{k}{c} \frac{\sqrt{1 + (1/\omega\tau)^2}}{\sqrt{\left[1 - \left(\frac{\omega}{\omega_0}\right)^2\right]^2 + \left(\frac{\omega}{\omega_0}\right)^2 \left(\frac{\omega_0 a}{c} + \frac{1}{\omega_0 \tau}\right)^2}} \quad . . (3)$$

where ω_0 is the natural frequency of the freely-vibrating system. This equation gives the "numerical amplitude" $A/k/c$ as a function of the "numerical frequency" ω/ω_0, the "numerical friction" $a' = \omega_0 a/c$, and "the numerical time of decay" $\tau' = \omega_0 \tau$.

Discussion of the relation 3

In *fig. 2* the numerical amplitude is plotted as a function of the numerical frequency for a specific case ($\tau' = 20$, $a' = 0.45$). The frequency scale ω/ω_0 has been divided into four regions which will be discussed separately.

I) Decay Region

At low frequencies the amplitude becomes very great owing to the decay of the restoring forces. If the frequency is so low that ω/ω_0 is small as compared with unity, we get from equation (3) for the numerical amplitude:

$$\frac{A}{k/c} = \frac{1}{\omega\tau} \quad . . . . . . (4)$$

It is therefore determined by the time of delay τ, and for this reason this region will be termed the decay region.

II) Static Region

In the region between approx. $^1/_{20}\,\omega_0$ and $^1/_2\,\omega_0$ the amplitude differs but little from the value:

$$A = k/c \quad . . . . . . (5)$$

This is Hooke's law, which applies to the static loading of a material with elastic constant c with a force k This region can therefore be termed the static region.

III) Friction Region

At resonance ($\omega = \omega_0$) the amplitude in the absence of friction would increase without limit. Friction limits the amplitude in such a way that the maximum numerical amplitude is inversely proportional to the numerical friction:

$$\frac{A}{k/c} = \frac{c}{\omega_0 a} = \frac{1}{a'} \quad . . . . . . (6)$$

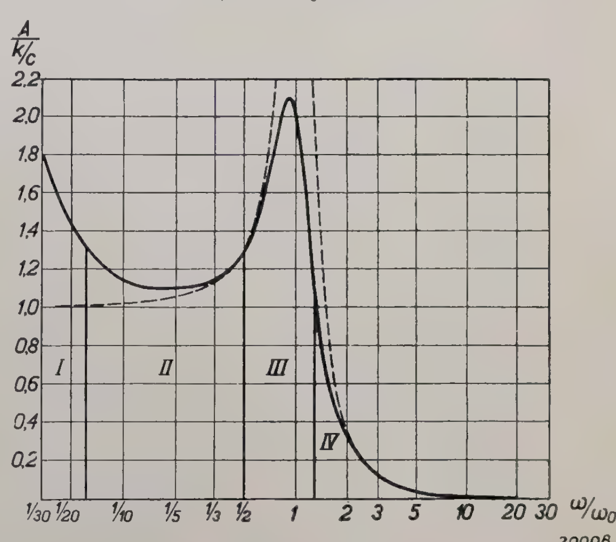

Fig. 2. Amplitude of a vibrating system as a function of the frequency when under the action of a constant energising force. At very low frequencies, the amplitude becomes very great owing to flow phenomena (decay of the restoring forces), while for the rest the usual curve for damped oscillations is obtained. The curve applies for $\omega_0 \tau = 20$, $\omega_0 a/c = 0.45$. *I* decay region; *II* static region; *III* friction region; *IV* mass region. The broken line shows the amplitude, in regions *I* and *III*, in the absence of friction and decay. In the latter case the amplitude at the resonance frequency becomes infinite.

IV) Mass Region

At very high frequencies $\omega \gg \omega_0$, the amplitude of the vibration becomes independent of the friction, the time of decay and the hardness of the spring. For this limiting case we get:

$$A = \frac{k}{c}\frac{\omega_0^2}{\omega^2} = \frac{k}{m\omega^2} \quad . \quad . \quad . \quad . \quad . \quad (7)$$

in other words a diminution inversely proportional to the mass and square of the frequency.

Equations (4) to (7) indicate that in each of the four frequency regions one of the four constants τ, c, a and m determines the amplitude. These results are collated in *table I.*

Table I

Region	Characteristic constant
I) Decay region	τ
II) Static region	c
III) Friction region	a
IV) Mass region	m

It is seen that the amplitude is determined in two regions (*I* and *III*) by the damping constants τ and a; the frequency range of these regions is proportional to $1/\tau$ and a. In the first region, that of decay, the decay of the restoring forces at a given amplitude of the forced vibrations leads to a reduction of the forces. In the third region (friction) the friction with given forces inducing vibration causes a reduction of the amplitudes.

A separate problem is the relationship between the damping constants on the one hand and the viscosity and decay of the damping agent on the other. This relationship cannot be immediately deduced, for it is governed by the method the vibrations are transmitted, particularly e.g. whether transversal or longitudinal vibrations are set up in the damping medium. A model for the pure transversal transmission of vibrations has been investigated theoretically and experimentally by Madelung and Flügge [3]).

Specific Applications

The above analysis indicates the existence of fundamentally different types of damping agents. The first type (flow-type damping agents) yields to slow displacements and is elastic with regard to high frequencies. These damping agents are particularly suitable for preventing the occurrence of elastic stresses on gradual deformation, e.g. in foundations. A typical example of this class of material is asphalt. Under a brisk blow from a hammer, which generates mainly high frequencies this material exhibits a true elasticity, but under a sustained pressure it commences to flow. The second group of agents (frictional damping agents) is elastic when subjected to slow displacements; the natural vibrations are, however, damped by internal friction. These agents are extremely suitable for damping instruments used for recording vibrations, particularly when the modulus of elasticity of the damping material is sufficiently small. Rubber is a typical frictional damping medium provided the impressed force is not too great, but also has a comparatively high modulus of elasticity, so that its use in vibrating systems considerably increases the rigidity in addition to the damping force.

A damping medium without this disadvantage has been employed in the sound recorder of the Philips Miller system. In this case the material has to be run into the damping chamber as a fluid and must then rapidly set, before it has a chance to flow into the air gaps of the magnetic system. These considerations, together with the need for a low modulus of elasticity, led to experiments being conducted with gelatinised systems, of which gelatin and agar-agar solutions are typical examples. Compared to fluid damping agents, a solid damping medium offers the advantage that the point of application of the damping force can be chosen arbitrarily and made of limited dimensions, and that the damping material can be applied directly where required in every case.

Mixtures of gelatin and water are unsuitable, as they rapidly dry out and also shrink considerably, so that on drying the material becomes detached from the walls. Both disadvantages can be overcome by the addition of glycerine. But a considerable amount of glycerine has to be added, which in its turn reduces the damping force too much. By adding water-soluble oils, the desired combination of a high damping and low rigidity was indeed realised, but at the same time the durability of the mixture was unsatisfactory, for in course of time shrinkage occurred and the rigidity increased.

The addition of sugar was found satisfactory from every point of view. The damping was increased, the rigidity remained small, and all shrinkage disappeared, while the adhesion of the material was excellent.

[3]) E. Madelung and S. Flügge, Ann. Physik, **22**, 209, 1935.

The damping properties of this material may be improved by a suitable thermal treatment. It is remarkable that this implies a diminuation of the viscosity of the mass in the liquid phase. Therefore the damping properties of definite gelatinising systems cannot be deduced as a rule from the properties of the system above the gelatinising temperature in the molten state.

The total damping of the sound recorder was roughly doubled by using this damping medium, while the sensitivity was reduced by only about 5 per cent.

By varying the composition, the physical properties of the material, such as melting point, damping, rigidity, could to some extent be modified. The addition of agar-agar in place of gelatin, for instance, raises the melting point.

It should be mentioned that this damping compound can also be employed for other damping duties, such as occur in wax-disc cutters and loud-speakers. One of the authors has used the damping agent described here with complete satisfaction for filling bicycle tyres, which thus acquired marked damping properties and no longer required pumping up. Since the compound does not flow, the cycle can be left to stand for a long time without the tyres going flat.

PRACTICAL APPLICATIONS OF X-RAYS FOR THE EXAMINATION OF MATERIALS VIII

By W. G. BURGERS.

In article No. VII of this series it was shown that the expansion (or contraction) of a crystal lattice is exhibited in X-ray analysis by a displacement of the interference lines towards a smaller (or larger) angle of deflection with reference to the direction of incidence. This phenomenon can be employed as the basis for a method for revealing the elastic strains in a material by means of X-rays [1]). These strains produce elastic deformations resulting in a slight change in the interatomic distances which alteration can be brought out by radiography. According to the nature of strain distribution in the material or workpiece this can happen in different ways. In general the strains vary in direction and magnitude from area to area. If the areas of nearly constant strain are greater than the cross-section of the X-ray beam (i.e. greater than about 1 sq mm) then the distortion of the lattice is the same throughout the whole of the irradiated area: The X-ray lines are then displaced either inwards or outwards according to the local strain. Strains of this type, which may be termed "macro-strains" may for instance occur in the neighbourhood of welded seams or in workpieces under an external load or stress, such as axles, levers, etc. Elastic strains may, however, vary over much smaller areas such that in a single square millimetre every possible state of strain can be found. Such micro-strains occur for instance in cold-worked (e.g. rolled) metals, even when these are not subject to external load. In such a case the inter-atomic distances in the irradiated area are slightly greater at one point and slightly smaller at another point: The X-ray lines are then displaced both inwards and outwards, so that the lines become indistinct, while their distance apart is to a first approximation the same as in the absence of any strain [2]).

Frequently the mechanical state of a workpiece will include both macro and micro-strains, a condition which is revealed in the radiograph by the presence of lines which compared with the radiograph for the unstrained material are displaced *as well as* broadened out.

To obtain the X-ray strain diagram for a workpiece the arrangement shown diagrammatically in *fig. 1* may be used with satisfactory results; here only those rays reflected in a direction almost opposite to that of the incident X-ray beam are registered on the film. This arrangement is favorable in view of the low value of the possible deformation. The maximum strains are indeed to a certain extent limited by the yield point (in certain circumstances

[1]) In certain circumstances it can also be measured, cf. A. E. van Arkel and W. G. Burgers, "Inwendige spanningen in metalen", Polytechn. Wbl. **28**, 513, 1934.

[2]) This has been demonstrated by W. P. Davey and A. E. van Arkel:
W. P. Davey, Gen. Electr. Rev. **28**, 586, 1925;
A. E. van Arkel, Physica **5**, 208, 1925.

by the ultimate strength) of the material, i.e. by the strain at which permanent set (or failure) is obtained. On exceeding the yield point the interatomic distances undergo on the average no further

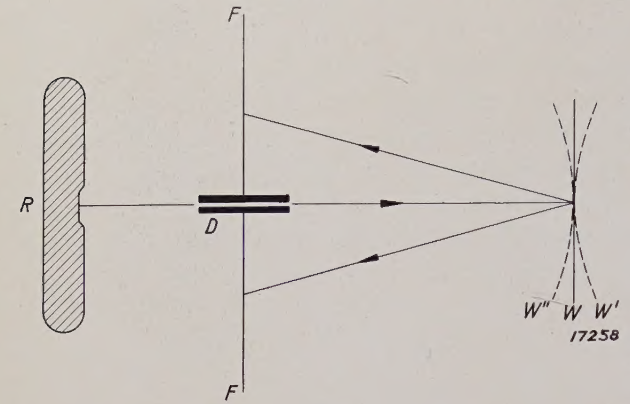

Fig. 1. Diagrammatic arrangement of X-ray tube, film and specimen for the X-ray investigation of internal strains.
R = X-ray tube. D = Diaphragm.
F-F = Photographic film (with a hole at the centre through which the diaphragm D projects).
W = Surface of workpiece or material under investigation (for the meaning of W' and W'' see example 17).

change over small areas of for instance 1000 atoms, since the lattice then gives and the atoms slide over each other. This critical strain, particularly with metals, is less than 1 per cent of the modulus of elasticity, in general being actually a much smaller fraction. The fluctuations in interatomic distances resulting from elastic strain will therefore be at the most of this order of magnitude, so that only the most sensitive lines on a radiograph will become measurably displaced, i.e. those lines which on a specific change in interatomic distance sustain the maximum displacement. As already indicated in the previous article (Philips techn. Rev. 1, 253, 1936: fig. 1*b*) these are the inner lines of a socalled "reversed" radiograph, i.e. a radiograph in which the film is so placed that the incident X-ray beam passes through a hole in the centre of the film. This method is employed in the arrangement shown in fig. 1.

As X-rays are strongly absorbed by metals, strain conditions can only be registered and investigated by the X-ray method which are located in the outer superficial layer (e.g. within a thickness of 20 μ) of the sample or workpiece under examination.

A number of simple applications of the X-ray method to the investigation of strain conditions are discussed below.

17. Detection of "Macro-strains" in an elastically-flexed Metal Strip

Fig. 2a shows the "most sensitive" interference lines in a radiograph of a rolled nickel-iron strip which was irradiated in a direction perpendicular to its surface W using the arrangement represented in fig. 1. *Fig. 2b* reproduces the radiograph of the same strip after it has been elastically flexed, as indicated by the hatched line W' in fig. 1 (the flexion between two points 4 cm apart being several millimetres). As a result of flexion the convex side of the strip has become elastically expanded parallel to the surface, and owing to transverse contraction it has become elastically constricted perpendicular to the surface.

The reduction in the interatomic distance in the latter direction causes a displacement of the sensitive X-ray lines inwards (see in particular the inner interference ring). If the band is flexed in the opposite direction (hatched line W'' in fig. 1) so that the X-ray beam strikes the concave side, there is a displacement of the lines in the opposite direction *(fig. 2c)*. Thus from an examination of the displacement of the lines, the character of the strains in the surface (and in certain circumstances also their magnitude, cf. the article in the Polytechn. Wbl. quoted) can be approximately determined. In the example under discussion here the line displacement can be equated against the strain produced by flexion, thus providing the basis of a method for determining the macro-strains at any point of a workpiece (e.g. in a welded seam); to do this it is merely necessary to compare the radiograph obtained with the arrangement shown in fig. 1 for the stressed area with the corresponding exposure obtained for an unstressed area.

18. Effect of Heat Treatment on the "Micro-strains" in a Steel Ring

The radiographs shown in *figs. 3a* and *b* were obtained with two steel rings of which one had been reheated to 600 ° C for half an hour. The definition of the sensitive interference lines (a doublet) is very different in the two exposures: in fig. 3*a* the lines are indistinct and in fig. 3b they are quite clearly separated. It may thus be concluded that the latter radiograph applies to the reheated ring: As a result of reheating the elastic "micro-strains" in this ring have disappeared, being retained in the non-heated ring (produced probably as a result of previous working) where they are indicated by the lack of definition in the interference lines.

19. Difference in Micro-strains between the Surface Layer and Core of a drawn Tungsten Wire

Fig. 4a reproduces the "most sensitive" X-ray lines of a radiograph prepared from a cold-drawn

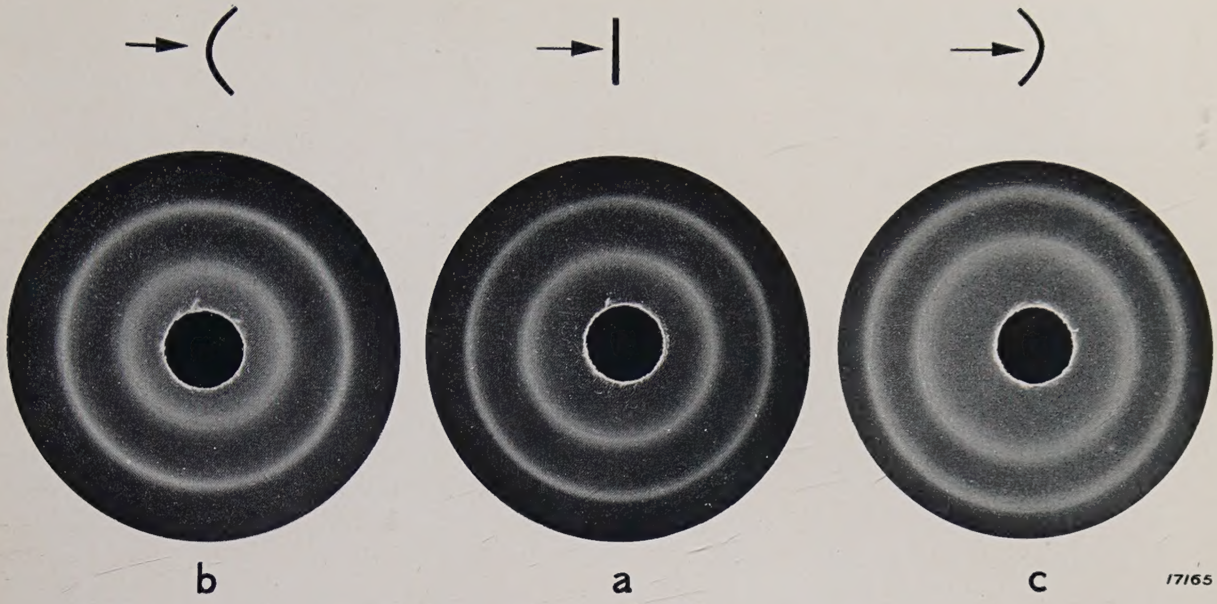

Fig. 2. Radiographs of a nickel-iron strip irradiated perpendicularly to the surface.
a Band flat . . . . (W in fig. 1).
b Band flexed, outer surface irradiated (W' in fig. 1).
c Band flexed, inner surface irradiated (W'' in fig. 1).

fine-crystalline tungsten wire 500 μ in thickness, while *fig. 4b* gives the corresponding lines for a radiograph of the same wire after etching off the skin to a depth of about 15 μ. The lines in fig. 4*a* lack definition, while those in fig. 4*b* are sharply defined (this is particularly shown by the fact that the pictures consist of two doublets whose separation is very different in figs. *a* and *b*). It may be concluded from these radiographs that the outer layer of a drawn tungsten wire, i.e. the layer which has come in direct contact with the drawing disc, has bene subjected to variable deformation from point to point [3]).

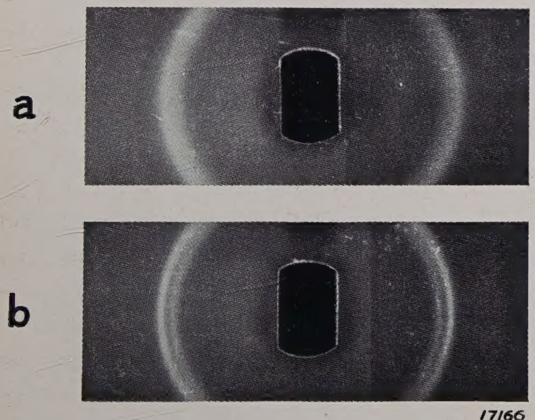

Fig. 3. Effect of heat treatment on the "micro-strains" in a steel ring.
a Non-reheated ring.
b Ring after reheating to 600 ° C for about half an hour.

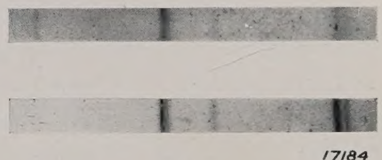

Fig. 4. Difference between the "micro-strains" in the outer layer and core of a drawn tungsten wire.
a Surface of unetched wire 500 μ thick.
b Surface after etching off a layer 15 μ thick.

[3]) As will be shown later, X-ray lines which lack definition can also be produced by the pressure of extremely small crystallites. This factor is probably of no moment in the present case, since the lack of definition in the lines can be eliminated in the radiograph of the unetched wire by reheating the wire to a temperature at which crystalline growth (recrystallisation) is still almost completely absent, although such atomic displacement occurs that the distortions of the crystal lattice and hence also the "micro-strains" are reduced.

ABSTRACTS OF RECENT SCIENTIFIC PUBLICATIONS OF THE N.V. PHILIPS GLOEILAMPENFABRIEKEN

No. 1114a: J. W. Roodenburg: Aardbeien onder neonlicht (Tuinderij, **16**, No. 25, June, 1936).

Practical data are given of the results achieved in strawberry culture with neon irradiation (cf. also Philips techn. Rev. **1**, 193, 1936).

No. 1115: J. A. de Vriend: Eine Methode zur Messung der Zündverzögerung von Blitzlampen (Z. wiss. Photogr., **35**, 129 to 131, June, 1936).

A method is described for measuring the lag on ignition of flashlight lamps using a cathode-ray oscillograph (cf. also Philips techn. Rev. **1**, 289, 1936).

No. 1116: P. G. Cath and O. L. v. Steenis: Der Ausdehnungskoeffizient von Barium und Kalzium und Allotropie (Z. techn. Phys., **17**, 239 to 241, July, 1936).

If liquid barium is cooled in a quartz tube of only medium thickness, the tube is found to fracture frequently. This behaviour indicates a change in modification of the barium in this temperature range. Between 0 and 300 °C. the linear coefficient of expansion was observed to be closely dependent on the thermal pre-treatment, and was 170 to $210 \cdot 10^{-7}$. After heating for two hours at 400 °C, the coefficient of expansion was approx. $182 \cdot 10^{-7}$. On heating to above 390 °C a considerable reduction in volume takes place which indicates a change in modification at this temperature. For calcium a coefficient of expansion of approx. $220 \cdot 10^{-7}$ was found below 300 °C, no transition temperature was observed with this element.

No. 1117: N. Warmoltz: A second sheath near the cathode of an arc discharge (Nature **138**, 36, July, 1936).

Between the Langmuir electrical double layer at the cathode and the light of the plasma of the arc a new, sharply defined layer has been discovered, which for various rare gases and mercury vapour is desciibed in this shoit communication.

No. 1118: A. Bouwers and J. H. van der Tuuk: A new X-ray tube for 700 kV and some measurements of penetrating radiation (Brit. J. Radiol. **9**, 431 to 441, July, 1936).

A description is given of a new sealed X-ray tube for voltages up to 700 kV. Two tubes for 400 kV are separately evacuated, then connected in series and joined while maintaining the vacuum. Some details are also given on the new high-tension equipment for 2.5 million volts at 3 milliamps (cf. Philips techn. Rev. **1**, 236, 1936). In conclusion the results of measurement are given for the absorption of X-rays, generated with voltages from 400 to 600 kV, by copper, tin, tungsten, lead and uranium filters.

No. 1119: W. G. Burgers and J. M. Jacobs: Crystal structure of titanium (Z. Kristallogr. A **94**, 299 to 300, July, 1936).

β titanium which is stable above approx. 900 ° C. has a cubic body-centred lattice with two atoms per elementary cell. At a temperature just above the transition point, the length of the edge of the elementary cell is 3.32 Å.

No. 1120: W. G. Burgers: Electron-diffraction photograph of a random arrangement of "cross-grating" crystallites (Z. Kristallogr. A **94**, 301 to 305, July, 1935).

The occurrance of an electron diffraction image with asymmetrical intensity distribution in the interference rings is correlated with the diffraction pattern, obtained by the method of M. von Laue with monochromatic waves on a random arrangement of two-dimensional lattices (cross-grating lattices).

No. 1121: C. J. Bakker and C. J. Boers: On the influence of the non-linearity of the characteristics on the frequency of dynatron and triode oscillators (Physica **3**, 649 to 665, July, 1936).

Formulae are given for the amplitude and frequency of dynatron and triode oscillators with non-linear characteristics, in a form suitable for experimental verification. The results of experiments are found to be in very good agreement with the values obtained from the theoretical formulae.